Title
A SURVEY OF THE APPLICATIONS AND LIMITATIONS OF VARIOUS TYPES OF DETECTORS IN RADIATION ENERGY MEASUREMENT

Permalink
https://escholarship.org/uc/item/0kx9j37r

Author
Goulding, Fred S.

Publication Date
1964-02-18

UCRL-11302

University of California

Ernest O. Lawrence Radiation Laboratory

A SURVEY OF THE APPLICATIONS AND LIMITATIONS OF VARIOUS TYPES OF DETECTORS IN RADIATION ENERGY MEASUREMENT

Berkeley, California

[illegible]r meeting and Proceedings of
[illegible]th Scintillation and Semiconductor
Counter Symposium - Washington D. C.
February 27-28, 1964

UCRL-11302

UNIVERSITY OF CALIFORNIA

Lawrence Radiation Laboratory
Berkeley, California

AEC Contract No. W-7405-eng-48

A SURVEY OF THE APPLICATIONS AND LIMITATIONS OF VARIOUS TYPES OF DETECTORS IN RADIATION ENERGY MEASUREMENT

Fred S. Goulding

February 18, 1964

A SURVEY OF THE APPLICATIONS AND LIMITATIONS OF VARIOUS TYPES OF DETECTORS IN RADIATION ENERGY MEASUREMENT

Fred S. Goulding

Lawrence Radiation Laboratory
University of California
Berkeley, California

Abstract

This paper provides a collection of data relevant to the use of various types of semiconductor detector in nuclear spectroscopy and gives examples of the use of detectors in specific experimental applications. Basic data on absorption of various kinds of radiation in germanium and silicon are given, and these are related to the characteristics of different types of semiconductor detectors. A brief outline of the optimization procedure for the detector-amplifier system to obtain good energy resolution follows. Included in a brief review of applications of detectors are examples in the fields of α-particle spectrometry, high-energy particle reactions, and low-temperature nuclear alignment studies.

Introduction

Striking changes have occurred in nuclear spectroscopy in the past 15 years. Starting with the use of scintillation counters and the development of multichannel analyzers capable of utilizing the resolving power of these detectors, a whole new field of high-resolution spectroscopy has developed. Traditional particle energy-analyzing techniques have been largely supplanted by methods based on the measurement of electrical pulse amplitudes obtained from detectors. While the traditional particle-deflecting techniques (usually magnetic) are still superior in resolving power, detector pulse-amplitude measuring techniques possess distinct advantages, in greatly improved geometry in counting experiments, and in much lower cost. In recent months even the accuracy advantage of the older techniques is being challenged, and the near future may see further gains in this direction.

To exploit the advantages of the new technology it is necessary for the experimental physicist to recognize the correct detector and system for his particular purpose. He must also have sufficient knowledge of the techniques of optimizing the system to achieve best results. Unfortunately textbooks and university courses provide little help toward these objectives (except in the case of scintillation detectors, which receive little attention here), and the proliferation of solid-state detector types, each accompanied by its own batch of specialized papers, does not make things easier for the physics research worker. This paper represents an attempt to collect basic detector information which can be used by the experimental physicist to select the appropriate type of detector and achieve best results from detectors and associated systems. Unfortunately we must recognize that a research worker in one institution may be able to use the latest types of detector while a worker elsewhere might find it difficult to obtain "state of the art" devices. It is tempting to neglect the more recent devices, which are available to only a select few, but commercial exploitation of solid-state detectors is so rapid that we would then be restricting the usefulness of the paper to a period of a few months at the most. In these circumstances, I have chosen to discuss applications of detectors in nuclear spectroscopy at the Lawrence Radiation Laboratory, where the diversity of users is probably as large as in any laboratory.

In recent years the most significant advances in detector technology have occurred in semiconductor detectors, and these will dominate our discussion. However, it seems desirable to briefly point out recent advances in scintillation and gas ionization detectors. In the latter, a considerable improvement in energy resolution has been reported by Vorobyov,[1] using purified acetylene in a gridded ion chamber. This work is of interest owing the large sensitive area possible with ion chambers and the absence of radiation damage (which can be a severe disadvantage in some applications of semiconductor detectors).

In scintillation counters, two recent developments offer the possibility of improved results, particularly in low-energy x-ray measurements. Hofstadter et al. report the use of CaI_2 as a scintillator producing twice as great a light output signal as NaI(Tl).[2] Landis reports on the use of a Philips XP1010 phototube and NaI(Tl) scintillator together with a noise-rejection system to give better than 50% resolution and very low counting rates due to noise for x-ray energies as low as 5.9 keV.[3] Combining the CaI_2 scintillator with the XP1010 phototube may well yield energy resolution in the 30 to 40% range at 5 keV. Semiconductor detectors and amplifier systems generate many noise pulses in this very-low-energy region, and scintillator-phototube combinations probably will continue to dominate this area of work. Major improvements in γ-scintillation detector resolution at high energies seem unlikely, as a substantial part of the 7 to 9% spread commonly observed in the range 500 keV to 1 MeV appears to be due to a physical effect in the scintillator.[4, 5] Although the only measurements of this phenomena are restricted to NaI(Tl), similar effects probably occur in other scintillators.

With these brief remarks on other types of detector we turn our attention to semiconductor detectors. The advantages of other kinds of detector in certain specific applications will be apparent as we examine the limitations of semiconductor detectors, but the general picture will be one of a rapid replacement of other kinds of detectors in many areas.

The Energy Conversion Process in a Semiconductor Detector

The primary advantage of semiconductor over scintillation and gas detectors lies in the improved efficiency with which particle energy is converted into an electrical signal. In the electronic system containing detector and amplifier, noise sources are present and the accuracy of measurement of the size of signals produced by the passage of nuclear particles through the detector is directly related to the ratio of the real signal to the noise. Charge produced in a semiconductor detector by absorption of a given amount of energy is about ten times that produced in a gas detector and, as one might expect, the energy resolution of the semiconductor detector system (i. e., the signal amplitude spread introduced by noise) can be about ten times as good as the gas detector system. In a scintillation detector the behavior is complicated by inefficiency of the process whereby particle energy absorbed by the scintillator is converted first into light photons, then into electrons emitted by the photocathode. This results in emission of a quite small number of photoelectrons, and statistical variations in this number produce considerable signal amplitude spread. Characteristic energy-resolution capabilities of the three kinds of detector might be as shown in Table I. Although these values are only approximate and represent specific cases, they serve to illustrate the advantages of semiconductor detectors over other types of counter for most nuclear spectroscopy applications.

The simplest method used to measure the energy of a γ-ray photon or nuclear particle consists of totally absorbing its energy in a detector and measuring the resulting signal. There are limits to the range of energies for which this is practicable, and the detector type must generally be chosen with these limits in mind. Since the ability of a detector to absorb radiation depends upon the physical properties of the material it seems appropriate to list here (Table II) some relevant properties of silicon and germanium, the only materials now used for detectors (and likely to be the only materials for some time to come).

The most extensive use of semiconductor detectors hitherto has been in particle spectroscopy. Using the information given in Table II and published range-energy data, one can calculate the range of various particles in detectors made of silicon and germanium. Range-energy curves are given for β particles (Fig. 1), protons, deuterons, tritons, helium-3, and α particles (Figs. 2 and 3) in silicon and germanium as also are the ranges in silicon of ions in the fission-fragment mass region (Fig. 4). The energy loss of particles in passing through thin slices of semiconductor is also important, partly owing to the unfortunate presence of a thin window at the entry port of detectors and also to the deliberate use of thin ΔE counters in particle identifying systems. Figures 5 through 10 show the energy loss in various thicknesses of silicon absorbers for β particles, protons, deuterons, tritons, helium-3, and α particles respectively. For minimum-ionizing particles (mesons, etc.), about 2 MeV is absorbed per g/cm^2 of absorber material.

In recent months interest has turned to the use of germanium and silicon at low temperatures for γ-ray spectroscopy.[6] We can theoretically determine the probability of γ-ray' s interacting with silicon or germanium by a photoelectric process, Compton scattering, or pair production, and can also determine the probability of escape of the annihilation quanta in pair production or of the degraded γ-ray in Compton scattering. As practical detectors are quite thin (< 1 cm) and do not contain high-Z elements, the probability of γ-ray interactions is quite small except at low energies. However, the energy resolution of semiconductor detectors can be about ten times as good as that of scintillation detectors, so that--despite the low efficiency and a much poorer photopeak/Compton ratio than with a NaI(Tl) scintillator--the ability to detect and identify peaks is much improved. Accurate calculation of the efficiency of semiconductor detectors for γ-ray measurements requires the use of a digital computer. However, approximate probabilities for γ-ray quanta of various energies to be totally absorbed in a detector 3 mm thick are shown in Fig. 11. This curve can be used only for general guidance, as the exact calculation has not been carried out. It should also be noted that allowance has not been made for escape probabilities of secondary electrons (which may produce a tail on the low-energy side of peaks in a spectrum) or for the escape probability of one or both annihilation quanta in the high-energy γ-ray region. At high energies most of the totally absorbed quanta shown in Fig. 11 appear as counts in the "double escape" peak (i. e., at an energy = E - 1.02 MeV) or the "single escape" peak (energy E - 511 keV).

Detector Types

The primary purpose of a detector is to absorb energy from the radiation quanta or particles and to produce an electrical signal proportional to the energy absorbed. The electrical signal is then amplified and sorted according to its amplitude. Unfortunately the detector and amplifier generate electrical noise, and there is also a possibility that physical processes in the detector may produce different output signals for the same energy absorption. The result of these imperfections in the detector and amplifier is to produce a spread in the signal amplitude; to minimize this spread, careful design of the detector and amplifier combination is necessary. In the detector the practical result of these considerations is to force the use of reverse-biased silicon p-n junctions if operation at room temperature is necessary, and of silicon or germanium p-n junctions if operation at low temperatures (liq. N_2) is allowed.

Table I. Typical energy-resolution values (full width at half maximum).

Energy	100 keV (β)	1 MeV (α)	10 MeV (α)	100 MeV (α)
Gas detector	30 keV	30 keV	30 keV	
Scintillation detector	15 keV	50 keV	200 keV	1 MeV
Semiconductor detector (25°C)	8 keV	10 keV	12 keV	50 keV
Semiconductor detector (77°K)	3 keV	7 keV	?	?

Table II. Properties of silicon and germanium.

	Silicon	Germanium
Atomic number	14	32
Atomic weight	28	72.6
Density (g/cm^3)	2.33	5.32
Dielectric constant	12	16
Energy gap (eV)	1.09	0.79
Energy per hole-electron pair	3.6	2.8
Electron mobility (25°C) (cm^2 V^{-1}/sec^{-1})	1350	3900
Electron mobility (77°K)	4×10^4 [a]	3.6×10^4 [a]
Hole mobility (25°C)	480	1900
Hole mobility (77°K)	1.8×10^4 [a]	4.2×10^4 [a]

a. Calculated values. To be regarded as approximate.

Probably the most important property to be determined before obtaining a detector for a particular experiment is its sensitive thickness. In particle spectroscopy this involves examining the appropriate range-energy relationship (Figs. 5 through 10) and selecting a detector whose thickness exceeds the particle range. If background counts are likely to be a problem, the detector thickness should be only slightly greater than the particle range (e. g., in high-background areas or in spectrometers in which weak samples are used).

An additional reason for selecting a sensitive thickness only a little greater than the particle range is of importance in high-energy applications. The charge-collection time in thick detectors is given approximately by

$$T = \frac{W^2}{\mu V}, \tag{1}$$

where T = collection time (sec),
μ = carried mobility (cm^2 V^{-1} sec^{-1}),
W = sensitive depth of detector (cm),
V = applied voltage.

Long collection time may cause charge loss by recombination, and may also prevent optimum adjustment of system parameters to give good energy resolution. Since the collection time is proportional to W^2, it appears desirable to reduce W to a minimum compatible with other requirements. On the other hand, a complication arises in very-high-resolution work, as the detector electrical capacity must have a low value to give good signal-to-noise ratio. The capacity is given approximately by

$$C = 1.1 \frac{k A}{4 \pi W} \text{ pF}, \tag{2}$$

where k = dielectric constant of detector material, and A = detector area (cm^2).

From this point of view the detector thickness should be as large as possible. The conflict between these requirements involves a compromise typical of the whole area of application of semiconductor detectors, and illustrates the need for careful choice of detector and electronics for each application. Before discussing the basis for compromise we will briefly review the types of detector that can be obtained.

Silicon-Diffused Junction Detectors

These detectors are made by diffusing a shallow layer of a donor (or acceptor) material into high-resistivity p-type (or n-type) silicon. The diffusant commonly employed is phosphorus, and p-type silicon in the resistivity range 100 to 10,000 ohm cm is used for the bulk material. The diffused layer can be very thin (< 1000 Å), but is more commonly in the 0.5-μ region. When positive voltage is applied to the n-type surface layer a depletion layer is formed in the bulk p-type silicon, the depth of the depletion layer (which is the sensitive region of the detector) being given by the equation

$$W = 0.32 \sqrt{\rho V} \text{ microns}, \qquad (3)$$

where ρ = resistivity (ohm cm) of the p-type material. Figure 12 shows a plot of this relationship and the equivalent one for n-type material. Note that the depletion layer for n-type material is deeper for a given voltage. Unfortunately n-type high-resistivity material is not so easy to obtain as p-type, and often contains mixtures of compensating impurities--a situation that may change at the high temperatures used in diffusion processes (≈ 1000°C). For this reason n-type materials are rarely used in diffused detectors.

The two electrical properties of most importance in detectors are the capacity [determined from Fig. 12 and Eq. (2)] and the leakage current, whose fluctuations contribute electrical noise to the system. The leakage current contains two components, one due to the thermally generated carriers in the depletion layer and the other due to surface effects where the edge of the junction reaches the surface of the silicon crystal. The second effect is usually dominant and, what is more, it varies greatly depending upon ambient conditions. Various methods, including the guard ring[7] and oxide surface protection,[8] have been developed to overcome this problem, and--in our experience--extremely reliable low-noise detectors can be made in substantial quantities with very high yield. The sensitive thickness of these detectors is limited to a maximum of about 600 μ (resistivity 10,000 ohm cm, voltage 500 V), but, apart from this limitation, these detectors are probably the most reliable and generally useful semiconductor detectors made at present. The thin uniform window and excellent energy resolution at room temperature make them useful for fission fragments, natural and machine-made (up to 40 MeV) α particles (resolution ≈ 15 keV for 1 cm^2), β particles (resolution 8 keV for 1 cm^2), and heavy ions. Improvements in these figures result if the detector is cooled.

This process is also well adapted to production of multichannel detector arrays on a single silicon blank. We have used a 100-channel array of this type for almost 2 years in an α-ray spectrometer.

Surface-Barrier Detectors

The basic principle of operation of the surface-barrier detector is the same as for the p-n junction, but the rectifying junction is between an evaporated gold layer and high-resistivity n-type silicon. Control of the parameters of this barrier is difficult to achieve, as the theory of barrier layers is not well developed. However, the depletion layer behaves similarly to that in a p-n junction (Fig. 12--n-type silicon) and it can be used as a particle detector. The method of manufacture of these detectors is very simple, involving no high-temperature processes, but in our experience, the yield of good detectors is low. It is possible to achieve thicker depletion layers in surface barriers (due to the use of n-type silicon) than in diffused junctions, but the yield of devices capable of the high-voltage operation necessary for these thick layers seems to be very small.

Lithium-Drifted Silicon Detectors

Equation (3) shows that the sensitive thickness of junction detectors is directly related to the resistivity of the bulk material, and very-high-resistivity material is necessary for thick detectors. Pell[9] showed that lithium (a donor) can be drifted into p-type silicon by applying, at a temperature in the range 100 to 150°C, reverse bias to a n-p junction consisting of a lithium-diffused n region on p-type silicon, and that the amount of drifted lithium adjusts itself so as to exactly compensate the acceptors in the bulk material. This results in the formation of a layer of very-high-resistivity material which grows from the n-type diffused layer into the p-type silicon. Drift time can be adjusted to control the thickness of this layer and a detector of known thickness can be produced. This is frequently referred to as a "n-i-p" detector.

If the drifting process is terminated before the whole thickness of the silicon slice has been converted to high-resistivity silicon, particles can enter the sensitive region only through thick windows (the original lithium diffusion might be 10 to 20 μ deep). It has therefore become common to initially cut the slice to approximately the desired detector thickness, then to drift lithium from one face (front) right through to the opposite face (back). The back is then etched and a gold surface barrier formed by evaporation. This surface barrier now constitutes a very thin window through which particles can enter the sensitive region of the detector. (This window is not so thin or so uniform as that in diffused or surface-barrier detectors).

Thickness limitations on these detectors are somewhat arbitrary. The drifting time is proportional to the square of the final thickness (typically 12 hours for 1 mm), and this leads to some restriction of thickness. Possibly more important is the increase in charge-collection time (Eq. 1) accompanying increasing thickness. If the detector is 3 mm thick and the applied voltage 300 V, the collection time is about 0.5 μsec at room temperature, and this increases rapidly as W increases. That the mobility of carriers increases as the temperature falls makes low-temperature operation attractive from this point of view. The use of high voltages (> 500 V) to reduce collection time is impossible owing to surface breakdown effects that cannot be eliminated with present techniques.

The usefulness of lithium-drifted silicon detectors at room temperature has been well demonstrated in their use in high-energy nuclear reaction experiments. They are also being used for β measurements, both at room temperature and lower temperatures (e. g., 77°K). Finally, they can be very useful for low-energy high-resolution γ-ray work when used at 77°K (see Fig. 11 for efficiency). The nonuniformity of the window thickness in these detectors detracts from their use for high-resolution work with heavily ionizing particles (e. g., natural α particles), and diffused or surface-barrier detectors should be used.

Lithium-Drifted Germanium Detectors

These are made by the same process as the lithium-drifted silicon detectors and are used at low temperatures (77°K), mainly for γ-ray spectroscopy. Unfortunately they, and--to a lesser extent--lithium-drifted silicon detectors suffer from surface problems. Extreme care must be taken to avoid surface contamination of germanium detectors.

Difficulties have been encountered in trying to make very thick lithium-drifted germanium detectors owing to the tendency of lithium to precipitate at vacancies and thereby to become electrically inactive. Our experience indicates that major problems occur for thicknesses greater than 3 mm, but detectors of this thickness can be produced relatively easily. However, they must be stored and kept at low temperatures (77°K) and in vacuum if they are to continue to be good detectors. Both surface problems and the precipitation phenomena probably contribute to make this necessary.

Selection of Detector

The choice of detector in many situations will be fairly arbitrary. However, in other cases, only one kind of detector can be used. For example, in γ-ray spectrometry efficiency considerations dictate the use of lithium-drifted germanium detectors (at 77°K) except at low energies, at which it becomes possible to use lithium-drifted silicon detectors (at reduced temperatures--240°K). Sometimes the thickness of detector required to stop the particles involved in the experiment will make the choice of detector obvious. For example, lithium-drifted silicon detectors are used for work with 60-MeV α particles. In other cases, the competing advantages and disadvantages of the various types of detector must be assessed carefully to make the best choice. For example, the thin window, room-temperature operation, and reliability of the diffused-junction detectors must be balanced against the high-resolution capabilities of lithium-drifted silicon detectors at low temperatures in consideration of which detector to use in a specific β-particle experiment. Here the choice may depend upon the importance of extremely good resolution ($\approx$ 3 to 4 keV with a lithium-drifted detector at 77°K, compared with $\approx$ 8 keV for a diffused junction at room temperature). In this and other cases the choice may be affected by consideration of the associated amplifier to which we now turn our attention.

Optimization of Detector-Amplifier System

We frequently hear the comment made by a physicist that the detector is noisy, or alternatively that the preamplifier is noisy. It seems to be very difficult to convince experimenters that there exists a mutual dependence between preamplifier and detector which makes it impossible to talk of one without reference to the other. In fact, a preamplifier that is optimized in design for one type of detector may not be appropriate for use with another detector, or for the same detector operating under different conditions. While the interrelation between detector, preamplifier, and amplifier constitutes a complex subject, it seems necessary to set down here certain basic principles for anyone attempting to achieve the best results with semiconductor detectors. We discuss the problems with particular reference to equipment in use at the Lawrence Radiation Laboratory, but the conclusions are applicable to equipment used in other laboratories.

At present we tend to divide our detector applications into four groupings:

(a) General-Purpose Moderate-Resolution Work. This includes work with fission fragments and medium-energy particles, for which extremely good resolution is not required. Here the general-purpose preamplifier front end (11X1051 P-1) shown in Fig. 13 is used together with the preamplifier output stages shown in Fig. 14. The virtue of this preamplifier is that it requires only low-voltage supplies available in the transistorized linear amplifier (11X1981 P-1) commonly used in these applications.

(b) Very-High-Energy Particle Moderate-Resolution Work. This includes nuclear reaction work with particle energies greater than 20 MeV. In this case, the same preamplifier is used as in (a), but the gain of the main amplifier is reduced to avoid noise at the main amplifier input from spoiling the energy resolution. This is necessary because the preamplifier output signal is deliberately attenuated at the main amplifier input when the signal input to the preamplifier is large.

(c) High-Resolution Work in which the Detector Capacity and Leakage Current are Large. In this case it is appropriate to use a tube having very high mutual conductance as the input stage to the preamplifier (11X1060 P-1, Fig. 13) despite the accompanying large input capacity and grid current. This preamplifier is commonly used with diffused junction detectors greater than 1/2 cm in diameter and with lithium-drifted silicon detectors when used at room temperature.

(d) Very-High-Resolution Work with Low-Capacity and Low-Leakage Detectors. In this case a low-capacity tube with low grid current and the highest possible mutual conductance (compatible with grid current and capacity) are chosen. This preamplifier (11X2950 P-1, Fig. 13) is used with low-temperature germanium and silicon lithium-drifted detectors.

Reference 7 gives full details of the theory involved in each specific case, but we briefly summarize the results of the calculations here in the hope the experimenter will find them useful in employing detectors. In most cases, noise sources not discussed in the reference become important as the optimum condition is approached, so the calculations can be used only as a general guide to optimum conditions. We assume that the main amplifier contains simple RC integrating and differentiating networks and, for the purposes of calculation, it is assumed that the RC time constants remain equal while being varied together over the range 0.1 to 10 μsec. The effect of electrical noise in a detector-amplifier system is to cause peaks to broaden and, for convenience, the following equation empresses the noise in terms of the full width at half-maximum (E_{FWHM}) of a monoenergetic line in a spectrum obtained by using a silicon detector. (If a germanium detector is employed the value of E_{FWHM} will be reduced by a factor 0.75.) Calculations given in reference 7 show that:

$$(E_{FWHM})^2 = 2\times10^{-2}\,\frac{C^2}{g_m T} + 2\times10^{-4}\,C^2 + 1.6\times10^{-1}\,T\,(i_g+i_L) + \frac{8T}{R}\,, \qquad (4)$$

where E_{FWHM} is expressed in keV,
C is the total input capacity in pF (detector and electronics),
T is the value of the integrator and differentiator time constants, expressed in μsec,
(i_g+i_L) is the sum of detector leakage and tube grid current expressed in nanoamperes,
R is the shunt resistance in the input circuit expressed in MΩ (detector load shunted by the grid resistors),
g_m is the mutual conductance of the input tube mmA/V.

For practical purposes the dominant terms in this equation are the first (tube shot noise) and third (current noise). The second, called flicker effect, is usually negligible in tubes chosen for preamplifier input purposes, and the final term can be made negligible compared with the third term by making R very much greater than

$$\left\{\frac{50}{(i_g-i_L)}\right\}\ \text{M}\Omega.$$

Figure 15 shows a plot of the two major terms of Eq. (4) for conditions that are typical in applications of two versions of the preamplifier shown in Figs. 13 and 14. The EC1000 tube is used in applications where the detector leakage and input capacity is small and the 7788 is used where the detector capacity and leakage are fairly large. At long time constants, the leakage and grid current noise is dominant, but at short time constants the tube shot-noise is most important. The dotted curves show the sum of the two contributions, and it is clear from these curves that an optimum amplifier time constant exists. In practice, one usually finds that other sources of noise cause a flattening of the valley in these curves, so that the amplifier time constant is not quite so critical as the curves suggest.

A final remark should be added about detector leakage current. In most simple detectors the leakage current is principally due to surface effects and these may or may not contribute electrical noise, depending on the precise nature of the surface. In good diffused-junction guard-ring detectors bulk leakage may be dominant and the theory given in Fig. 15 is fairly good. A similar situation may prevail in low-temperature applications of detectors.

Examples of Applications of Detectors in High-Resolution Experiments

Much of the low-energy physics program at the Lawrence Radiation Laboratory now depends upon semiconductor detectors for particle and γ-ray measurements. It is difficult to deal with the wide range of applications in a brief summary like this, but a few examples and some remarks on the limitations of the detectors may illustrate the application of earlier portions of this paper.

Fission Fragment Studies

Semiconductor detectors of the diffused-junction type provide a very simple means of measuring the energy of fission fragments and, in consequence, have completely replaced earlier techniques. Ideally the detectors should be made of low-resistivity silicon, as fission fragment ranges never exceed 25 μ (see Fig. 4). However, work on the oxide passivation technique[8] has so far been limited to resistivities > 400 Ω cm, and our fission fragment detectors have generally been in the 1000-Ω cm region. Fission fragment detectors should have very thin diffusions; we use 0.5 μ, but this will be reduced in the near future.

The major problem in this area arises from radiation damage effects in the detectors. We generally observe about 10^8 counts/cm^2 before degradation of the detector makes its replacement necessary. Some improvement in this behavior might be forthcoming if lower-resistivity silicon were used, but a simple calculation shows that the density of deposited fragments in the silicon lattice for 10^8 counts approaches the same value as the density of acceptors in the material. It therefore seems unlikely that a very large improvement can be made.

In general, fission fragment studies have not called for very high resolution. However, Harry Bowman has recently been studying the γ-rays emitted by fission fragments and observing Doppler shifts in the γ-ray lines according to the direction of the fragments.[10] For this purpose, a lithium-drifted germanium detector at 77°K was used together with the EC1000 preamplifier, and γ-ray signals were observed in coincidence with signals from two fission counters mounted at 180° with respect to each other. The γ-ray energy resolution in this experiment has ranged from 3.5 to 5 keV, depending upon γ-ray energy and the particular experimental setup.

High-Energy Nuclear Reactions

Lithium-drifted silicon detectors have been used extensively in the nuclear reactions work at the 88-inch cyclotron. This machine provides α-particle beams up to 120 MeV and protons up to 60 MeV. Thick detectors are used to absorb these high-energy particles, but experience has shown that the long charge collection times encountered in detectors much more than 2 mm thick prohibit their use in high-resolution work. If the surface problems that limit applied voltage could be eliminated, thicker detectors could be employed. Transmission counters (either "punched through," diffused junctions, or lithium-drifted silicon detectors) are frequently used for purposes of particle identification in these experiments.

Typical energy resolutions obtained are in the 0.2% region. For example, the FWHM of a 50-MeV peak might be 100 keV. That this is much larger than the expected detector-amplifier resolution (which is measured with a pulser) indicates that other sources of spread are present. Spread in the beam energy itself is believed to be smaller than this by about a factor of 5 (i.e., 0.04%), and we believe that the source of the extra spread is in the detector itself. Not enough work has yet been carried out on this problem, but trapping of carriers in the silicon might possibly provide the explanation.

In high-energy applications of detectors care must be taken to avoid the possibility that the noise in the main amplifier itself limits resolution. Our standard amplifier meets this requirement, but many older amplifiers do not.

The very low neutron sensitivity of semiconductor detectors as compared with scintillators permits the design of experiments that were virtually impossible previously. An experiment planned by George Igo uses this feature of semiconductor detectors to reduce the neutron background counting rate and thereby allows the observation of a very low rate of coincident events in counters observing scattered particles from a target.

Alpha-Decay Studies

The first reported uses of semiconductor detectors were for α-particle spectroscopy, and they continue to provide the best high-geometry measurements. An example of the excellent resolution available in the oxide-passivated junction detectors is shown in Fig. 16. This shows the fine structure in the Am^{241} α spectrum and also illustrates the absence of any spurious background in the spectrum. Note that the 5.534-MeV line is only about 1/200 as strong as that at 5.477 MeV.

Frank Asaro has recently been studying the γ-rays emitted during the α decay of Am^{242m}, and some of his results are shown in Fig. 18. The upper curve shows the γ-ray spectrum obtained with a lithium-drifted germanium detector and an Am^{242m} source contaminated with Am^{241} and Cm^{242}. The resolution of the system is illustrated by observing the double peak between channels 110 and 120. These lines are 4 keV apart. The lower curve shows the γ-ray spectrum in coincidence with counts in an α detector with energy selection on the α side to remove counts due to Cm^{242}. The wealth of detail in this curve illustrates the problem facing experimental physicists involved in analyzing the data !

It is interesting to note that the contributions of Am^{241} could also have been eliminated from the γ-ray spectrum but, owing to the very low activity of the source, Asaro was forced to place the source very close to the α detector. The effect of the 0.5-μ window was then to worsen the α energy resolution so that he found it impossible to select only the Am^{242m} α group. A thin-window detector would have improved this situation.

Beta-Ray Spectrometer

As the energy selection of a β-ray spectrometer is one or two orders of magnitude more accurate than that of a semiconductor detector, there appears at first sight to be no future for such detectors in this area. However, the low inherent background of semiconductor detectors as compared with the Geiger counters or scintillators used previously makes them extremely useful in measurements on weak sources. As an example, almost a 10-to-1 improvement in background at energies greater than 100 keV has been obtained in replacing a Geiger counter by a solid-state detector (at room temperature) in our spectrometer. The Geiger counter is still superior, however, at low energies, where the tail of the noise pulse spectrum produces counts when the semiconductor detector is used. Cooling the semiconductor detector would improve this.

Conversion Electron Studies

Some of the most exciting applications of β and γ-detectors used at low temperature to obtain good resolution are illustrated in Figs. 18, 19, and 20. The direct relationship between the γ rays emitted by Ce^{137m} and the conversion electrons is striking when one compares Figs. 19 and 20.

A further illustration of the use of detectors at low temperatures, in this case in nuclear alignment studies, is given in Fig. 21. Here the detector (a germanium surface barrier) is used at 1°K. At this temperature the germanium is almost intrinsic. Further work on counters at extremely low temperatures is required to obtain a better understanding of their behavior.

We have also used lithium-drifted silicon and germanium detectors at 77°K in Mössbauer experiments. Using a small germanium detector ($1\ cm^2$, 0.3 cm thick) and the EC1000 preamplifier, we have established what seems to be a record for high resolution--2.17 keV on a 60-keV γ-ray. Interestingly, the γ resolution of this detector at high energies was poor (9 keV at 1.2 MeV) although the resolution measured with a pulser remained good. This discrepancy is much more than can be explained by the statistics of hole-electron production and, as with very-high-energy particles, we are probably forced to invoke a trapping effect as a possible cause.

Acknowledgments

It is difficult to acknowledge all the contributions to this paper, but I should particularly like to thank Leo Schifferle, Richard Crow, Stuart Wright, Donald Landis, and Morris Roach, who prepared several of the figures. My thanks must also go to Frank Asaro, Dave Shirley, Bernard Harvey, and Stanley Thompson, and to members of their groups, for the data contained in the final part of the paper. Discussions with William Hansen have resulted in many of the ideas contained in this paper.

This work was carried out as part of the Atomic Energy Commission contract with the University of California and forms part of the program of the Nuclear Chemistry Division of the Lawrence Radiation Laboratory.

References

1. Private communication from A. Vorobyov (Ioffe Physical-Technical Institute, Leningrad, Russia) to Albert Ghiorso (Lawrence Radiation Laboratory).
2. R. Hofstadter, E. W. O'Dell, and C. J. Schmidt, CaI_2 and CaI_2 (Eu) Scintillation Crystals, paper 1.4 of this conference.
3. Donald A. Landis and Fred S. Goulding, The Application of Pulse-Shape Discrimination to Separating Phototube Noise Pulses from Scintillation Pulses, Lawrence Radiation Laboratory Report UCRL-11301, Feb. 1964.
4. P. Thieberger, E. C. O. Bonacalza, and H. Ryde, Experimental Determination of the Influence of Non-Proportional Response of NaI(Tl) Crystals upon the Resolution of Scintillation Detectors, in Proceedings of Symposium on Nuclear Instruments, Harwell, September 1961 (Academic Press, Inc. New York, 1962), p. 54.
5. P. Iredale, The Non-Proportional Response of NaI(Tl) Crystals to γ-Rays, Nucl. Instr. Methods 11, 336 (1961).
6. A. J. Tavendale, Semi-Conductor Lithium-Ion Drift Diodes as High-Resolution Gamma Ray Pair Spectrometers, paper 3.2 of this conference.
7. Fred S. Goulding and William L. Hansen, Leakage Current and its Influence on Energy-Resolution Characteristics, Lawrence Radiation Laboratory Report UCRL-9436, Nov. 1961.
8. William L. Hansen and Fred S. Goulding, Oxide-Passivated Silicon p-n Junction Particle Detectors, Lawrence Radiation Laboratory Report UCRL-11227, Jan. 1964.
9. E. M. Pell, Ion Drift in a n-p Junction, J. Appl. Phys. 31 (2), 291 (1960).
10. H. R. Bowman, S. G. Thompson, J. O. Rasmussen, Gamma-Ray Spectra form Spontaneous Fission of Cf^{252}, Lawrence Radiation Laboratory Report UCRL-11203, Jan. 1964.

Figure Captions

Fig. 1 - Range of electrons in silicon and germanium.

Fig. 2 - Range of p, d, t, He^3, and α in silicon.

Fig. 3 - Range of p, d, t, He^3, and α in germanium.

Fig. 4 - Range of fission fragments in silicon.

Fig. 5 - β-Particle energy absorption in thin silicon detectors.

Fig. 6 - Proton energy absorption in thin silicon detectors.

Fig. 7 - Deuteron energy absorption in thin silicon detectors.

Fig. 8 - Triton energy absorption in thin silicon detectors.

Fig. 9 - He^3 energy absorption in thin silicon detectors.

Fig. 10 - α-Particle energy absorption in thin silicon detectors.

Fig. 11 - Probability of absorption of γ-ray photons in silicon and germanium detectors 0.3 cm thick.

Fig. 12 - Depletion-layer depth for p- and n-type silicon.

Fig. 13 - Preamplifier input stages.

Fig. 14 - Preamplifier output stages.

Fig. 15 - Effect of circuit parameters on energy resolution.

Fig. 16 - Am^{241} α spectrum (diffused-junction detector).

Fig. 17 - Am^{242} γ-rays associated with α decay.

Fig. 18 - Low-energy conversion electron spectrum of Ce^{137m} (Li-drifted Si detector at 77°K).

Fig. 19 - γ-Ray spectrum of Ce^{137m} (Li-drifted Ge detector at 77°K).

Fig. 20 - High-energy conversion-electron spectrum of Ce^{137m}

Fig. 21 - Very-low-temperature (1°K) conversion-electron spectrum of Ce^{137m}.

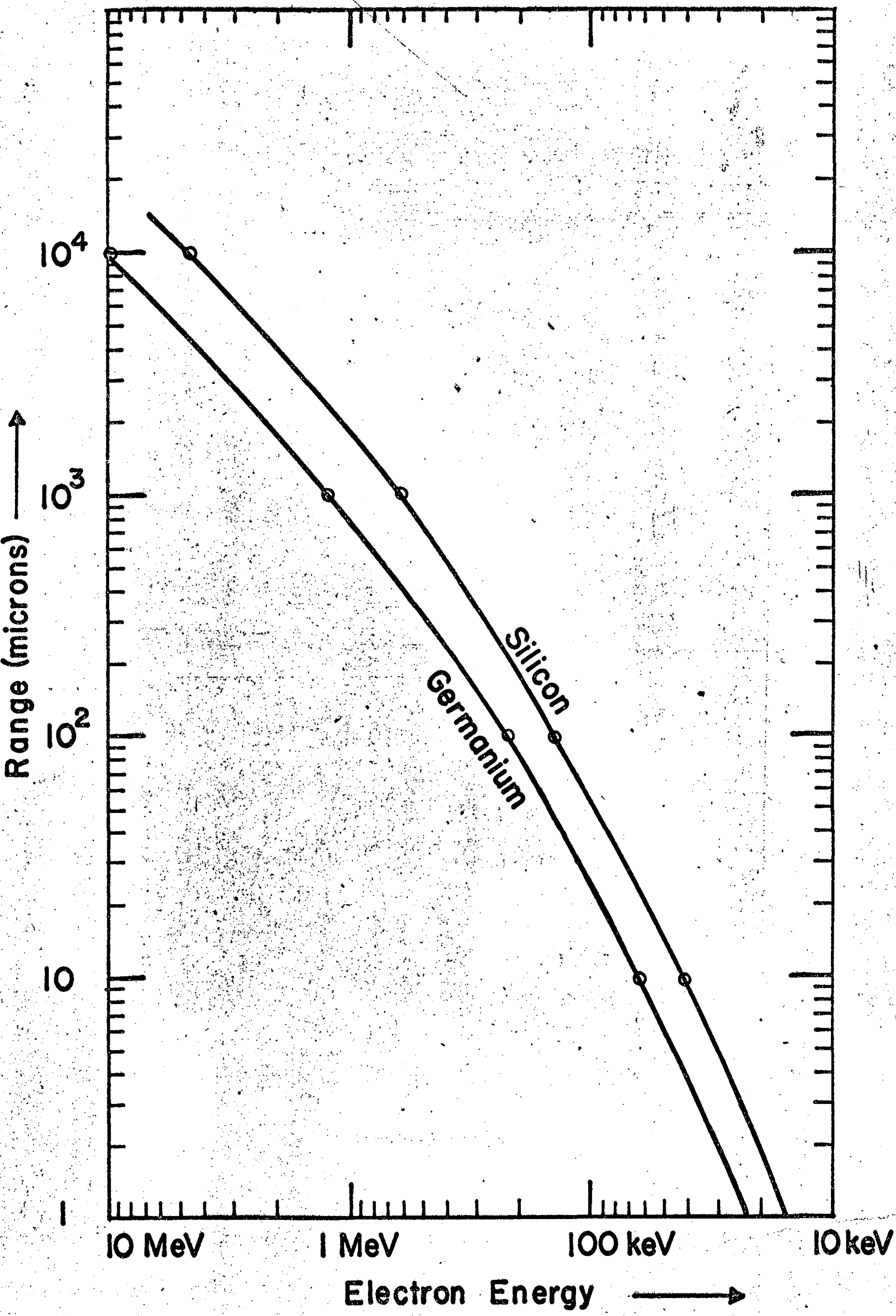
Range (microns)
10^4
10^3
10^2
10
1
10 MeV
1 MeV
100 keV
10 keV
Electron Energy
Silicon
Germanium

Fig. 1

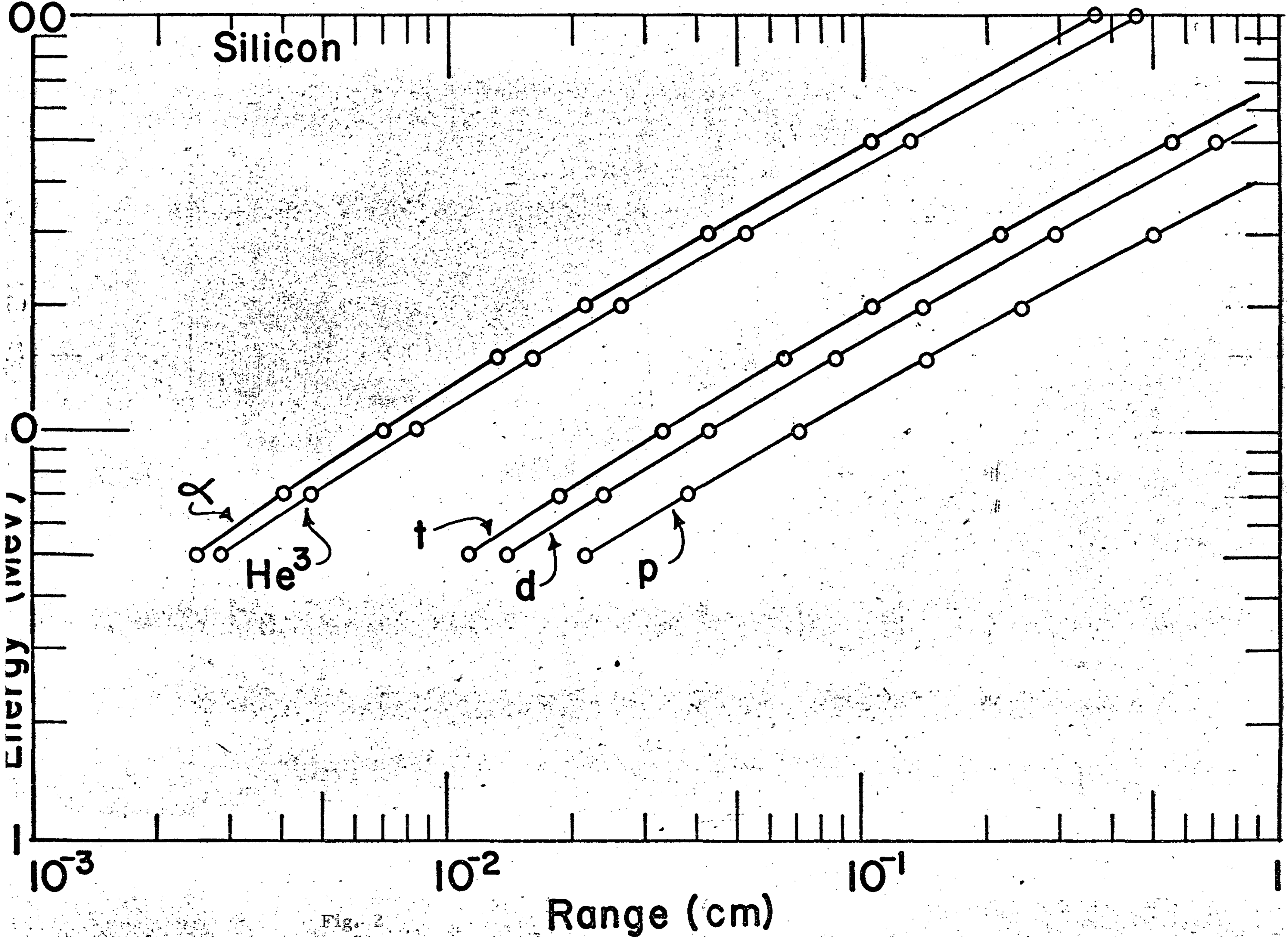

Fig. 2

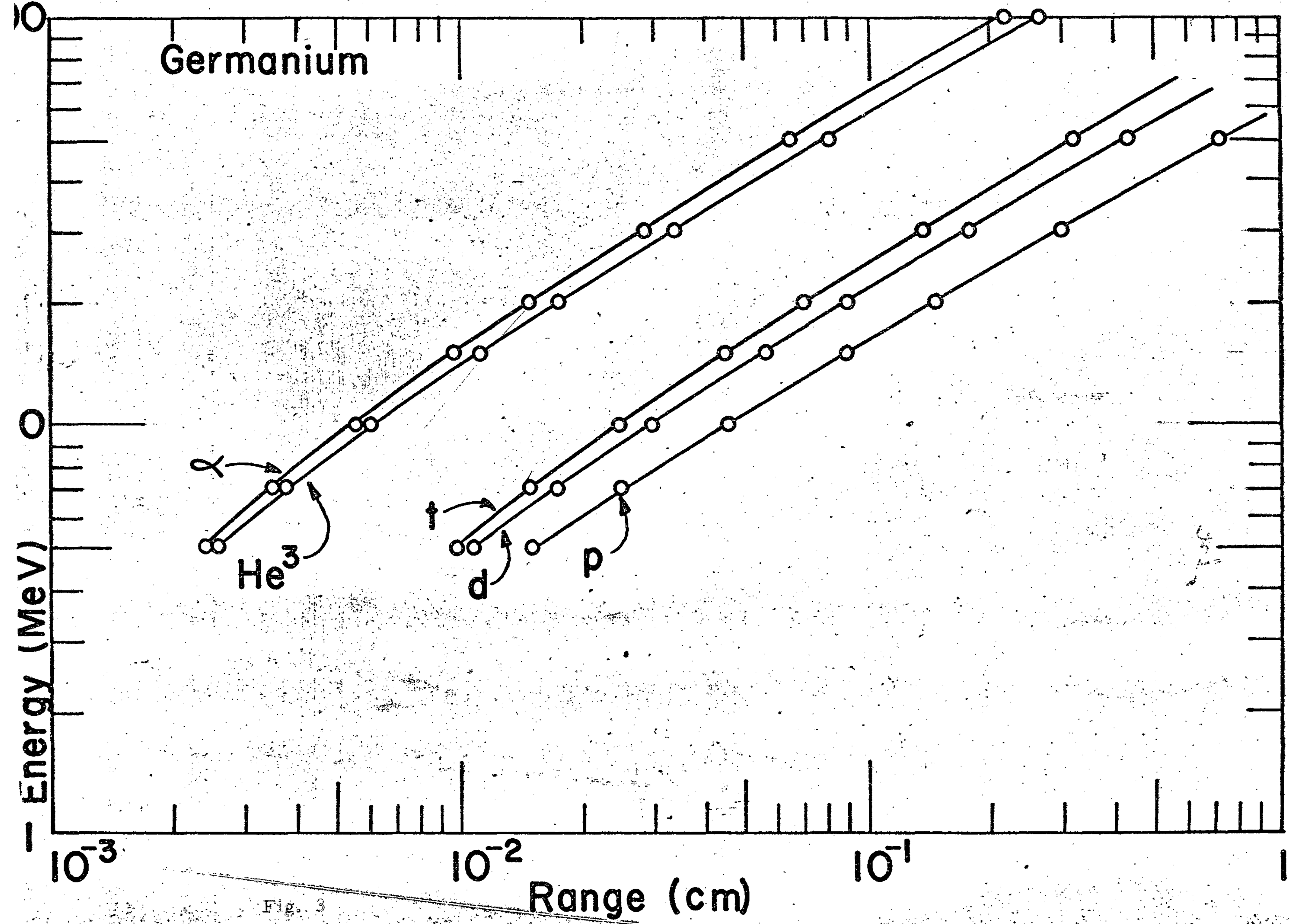

Fig. 3

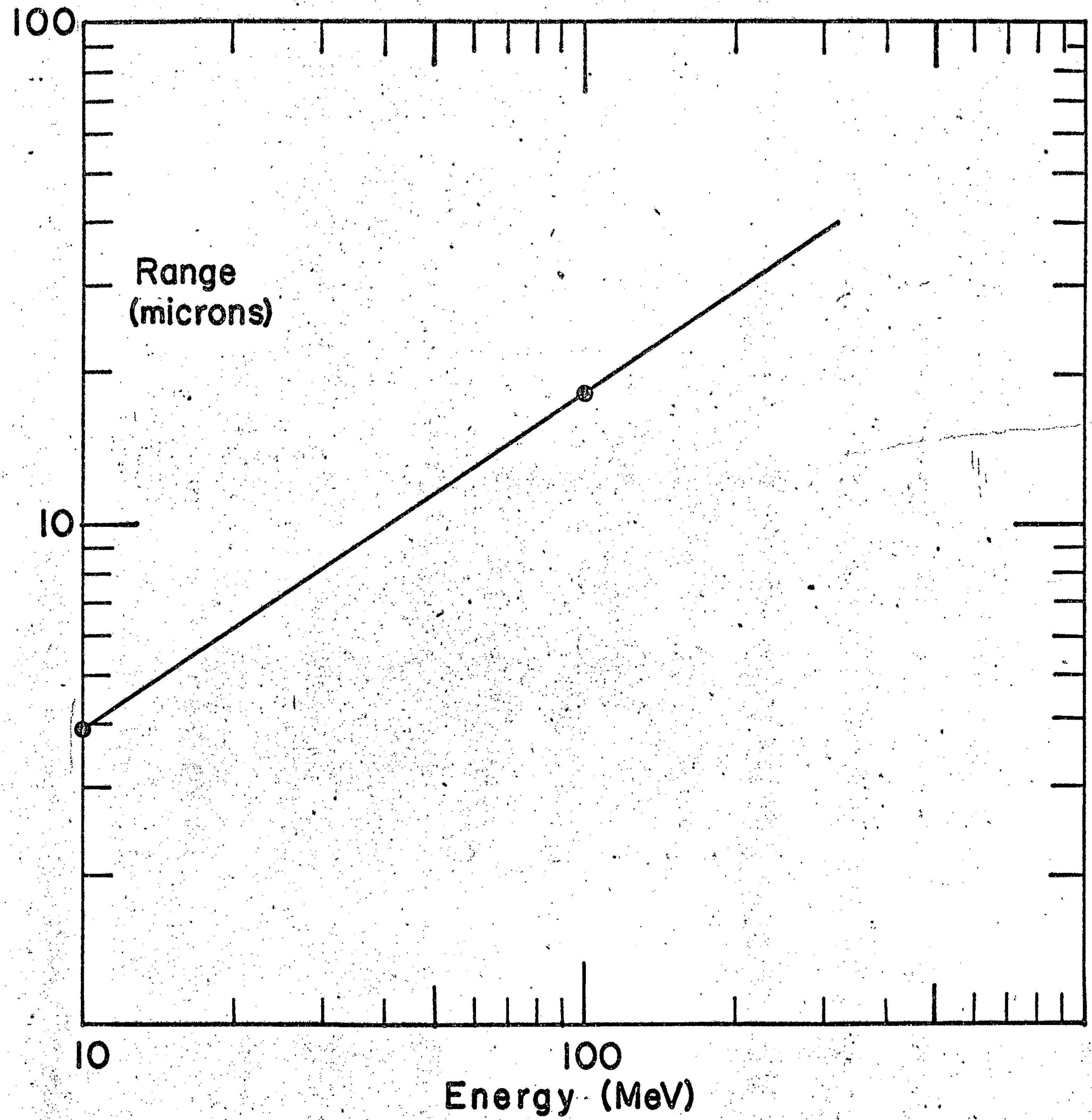

Fig. 4

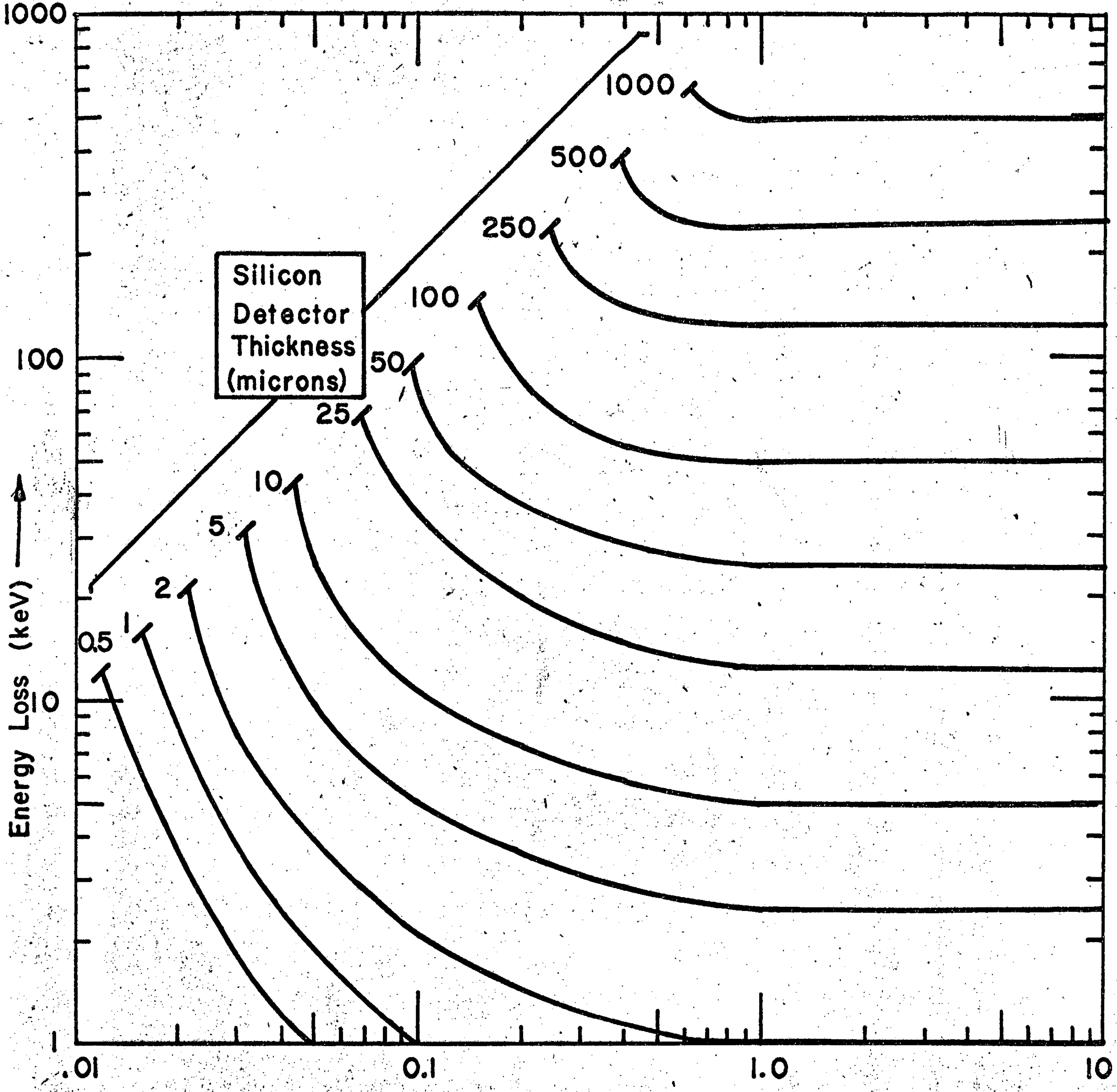
Silicon Detector Thickness (microns)
1000
500
250
100
50
25
10
5
2
1
0.5
Energy Loss (keV)
1000
100
10
1
.01
0.1
1.0
10
Electron Energy (MeV)

Fig. 5

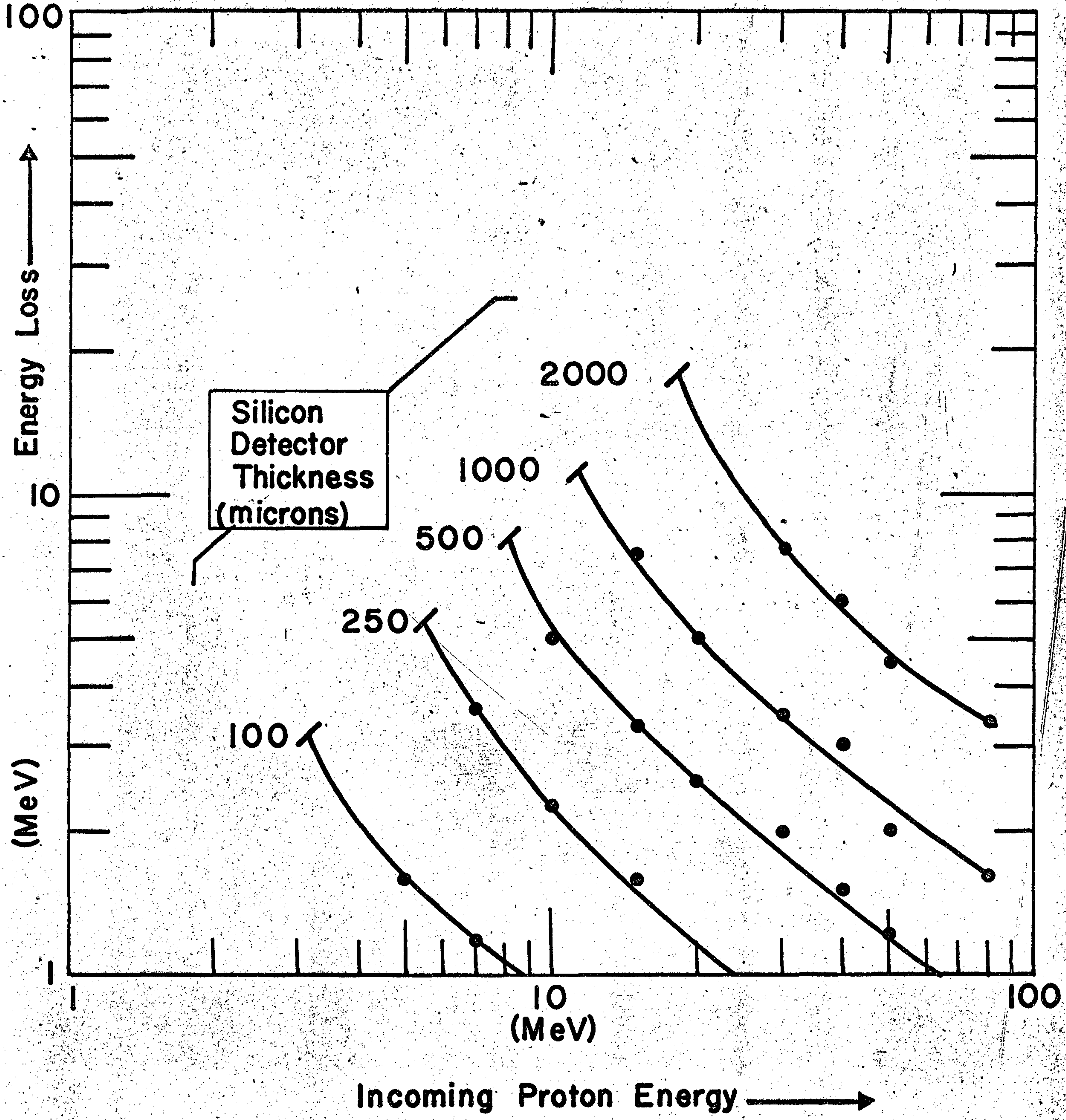
100
10
1
Energy Loss
(MeV)
1
10
100
(MeV)
Incoming Proton Energy
Silicon Detector Thickness (microns)
2000
1000
500
250
100

Fig. 6

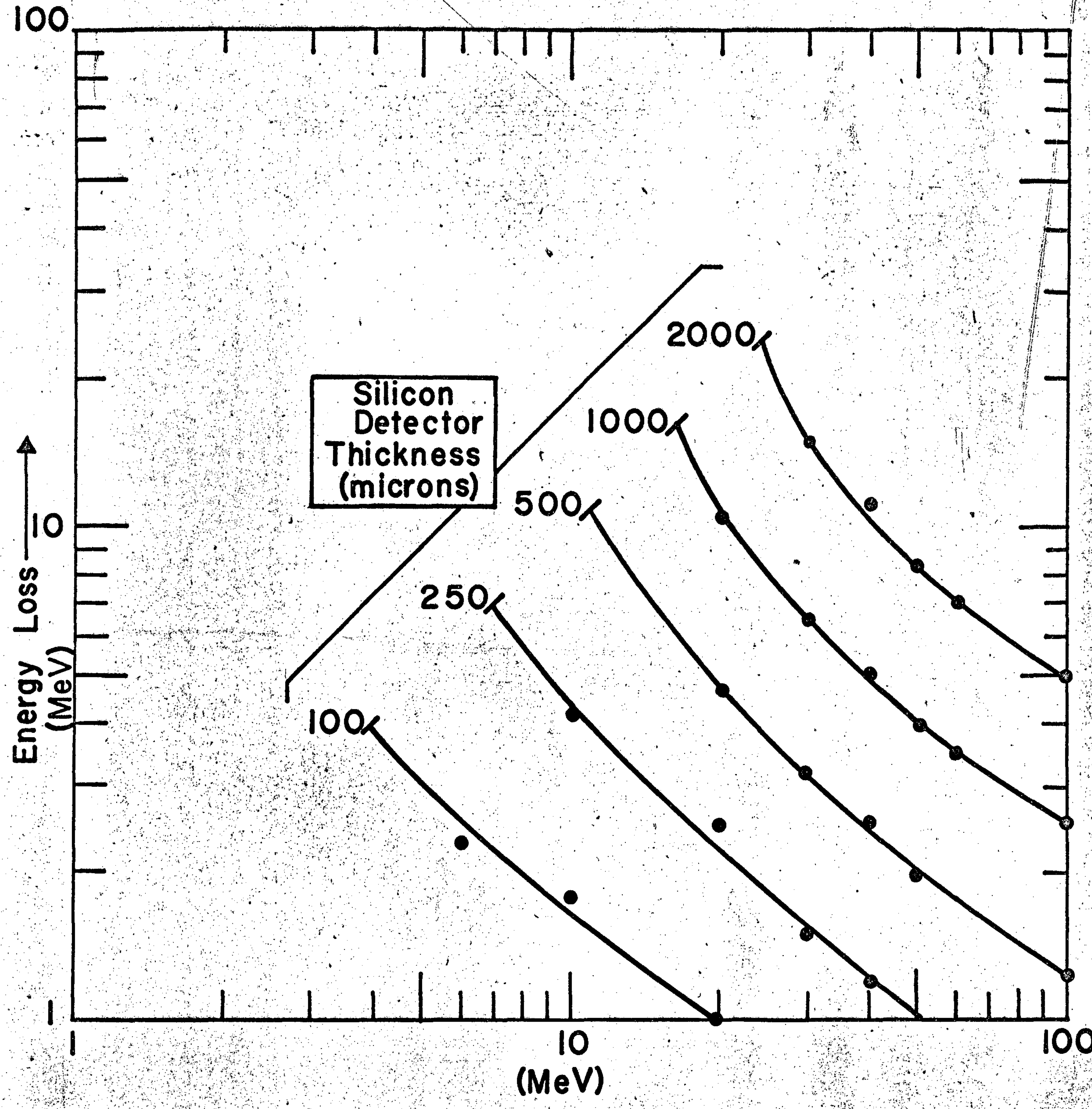
100
10
1
Energy Loss
(MeV)
1
10
100
(MeV)
Incoming Deuteron Energy
Silicon Detector Thickness (microns)
2000
1000
500
250
100

Fig. 7

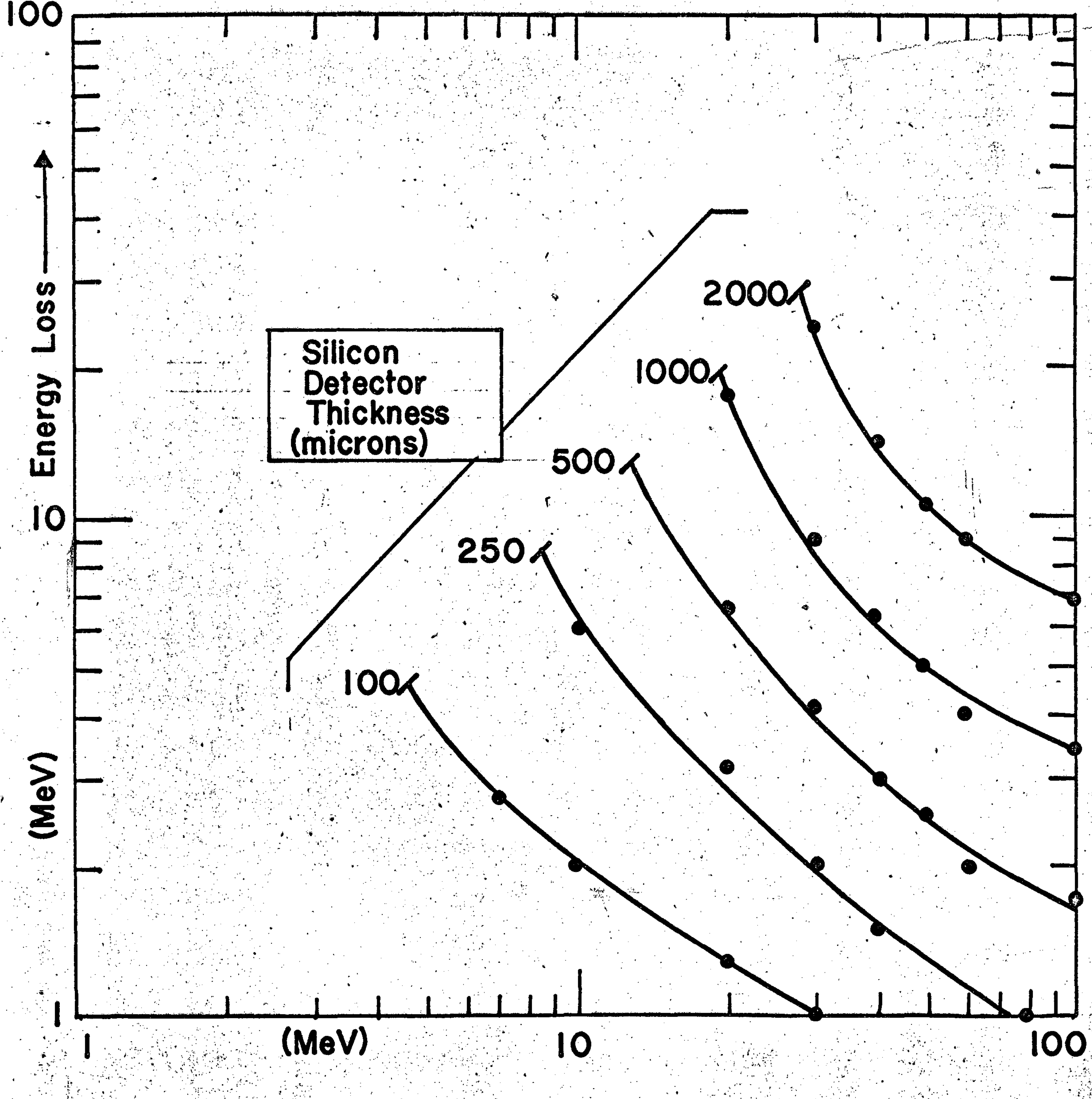
100
10
1
Energy Loss
(MeV)
Silicon
Detector
Thickness
(microns)
2000
1000
500
250
100
1
(MeV)
10
100
Incoming Triton Energy

Fig. 8

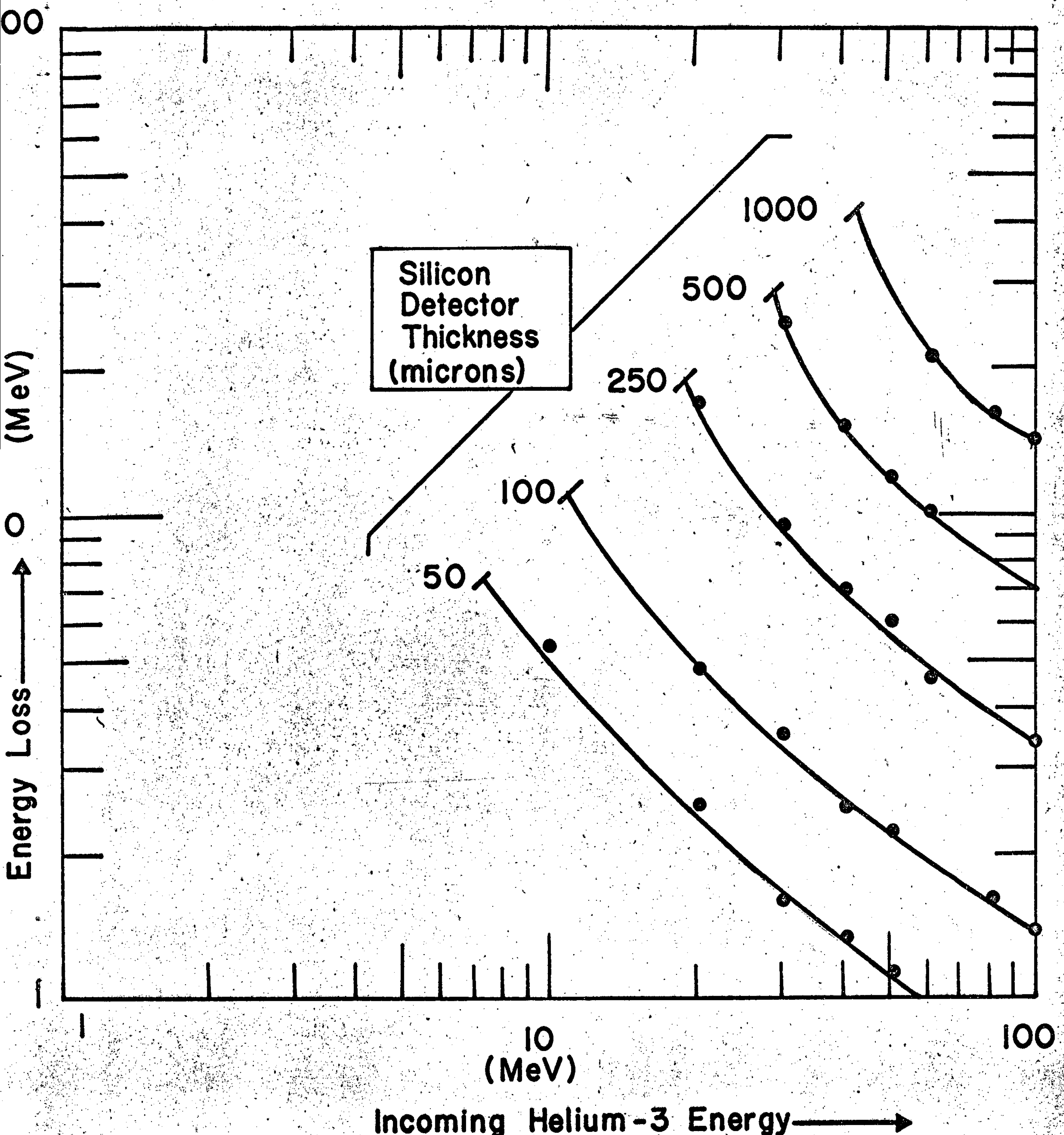
00
0
1
Energy Loss ⟶ (MeV)
1
10
100
(MeV)
Incoming Helium-3 Energy ⟶
Silicon Detector Thickness (microns)
1000
500
250
100
50

Fig. 9

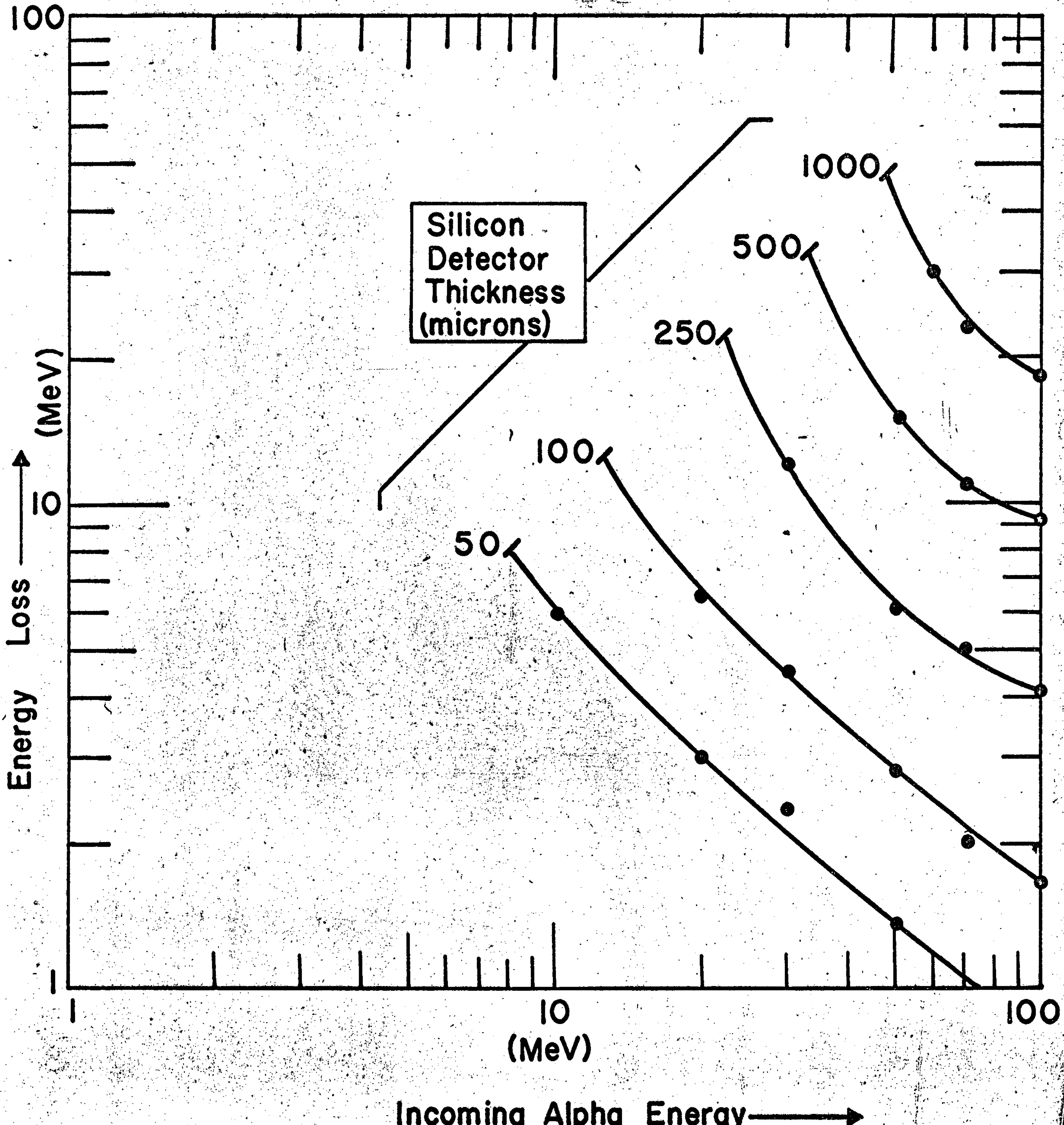
100
10
1
1
10
100
(MeV)
Energy Loss ⟶ (MeV)
Incoming Alpha Energy ⟶
Silicon Detector Thickness (microns)
1000
500
250
100
50

Fig. 10

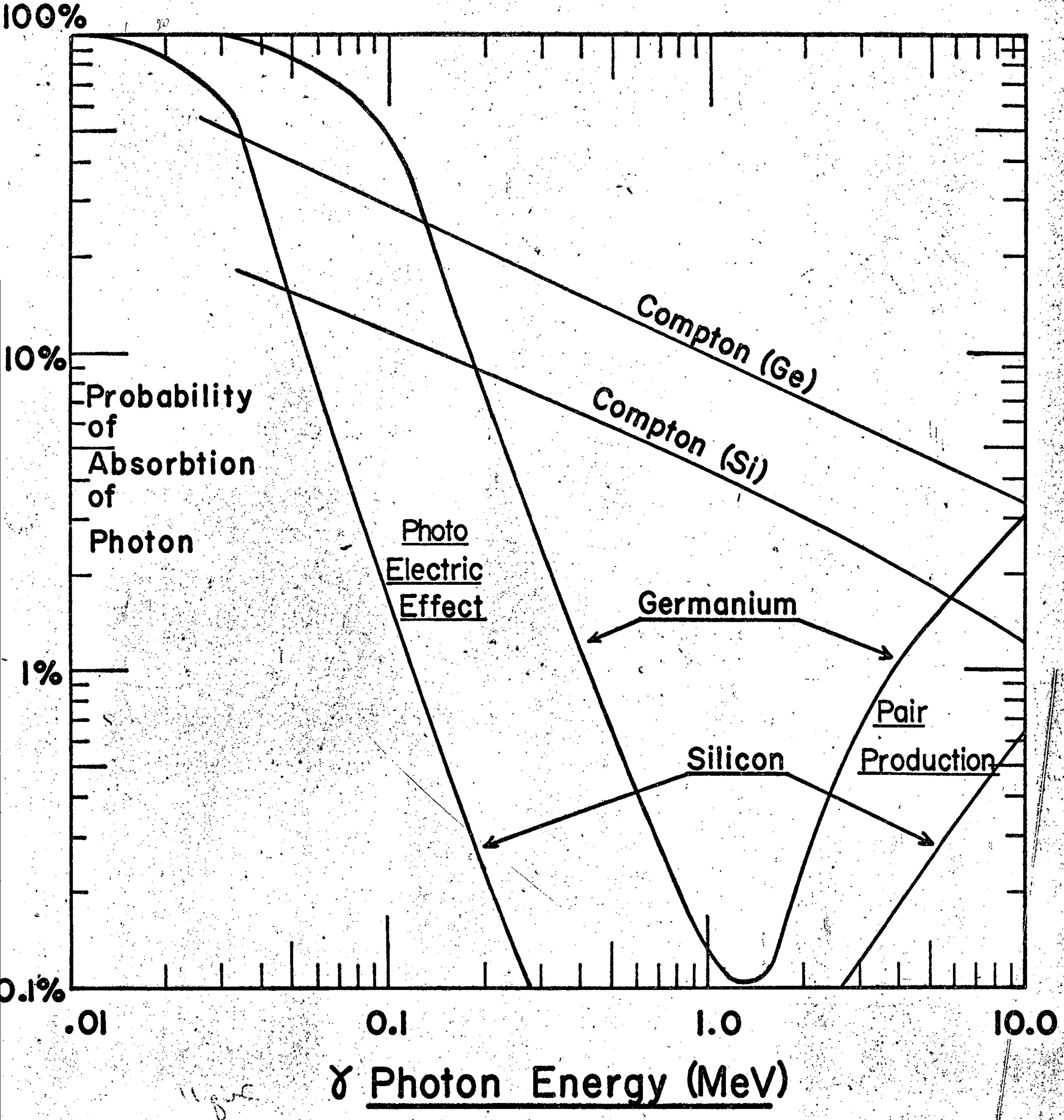
100%
10%
1%
0.1%
Probability of Absorbtion of Photon
Compton (Ge)
Compton (Si)
Photo Electric Effect
Germanium
Silicon
Pair Production
.01
0.1
1.0
10.0
γ Photon Energy (MeV)

Fig. 11

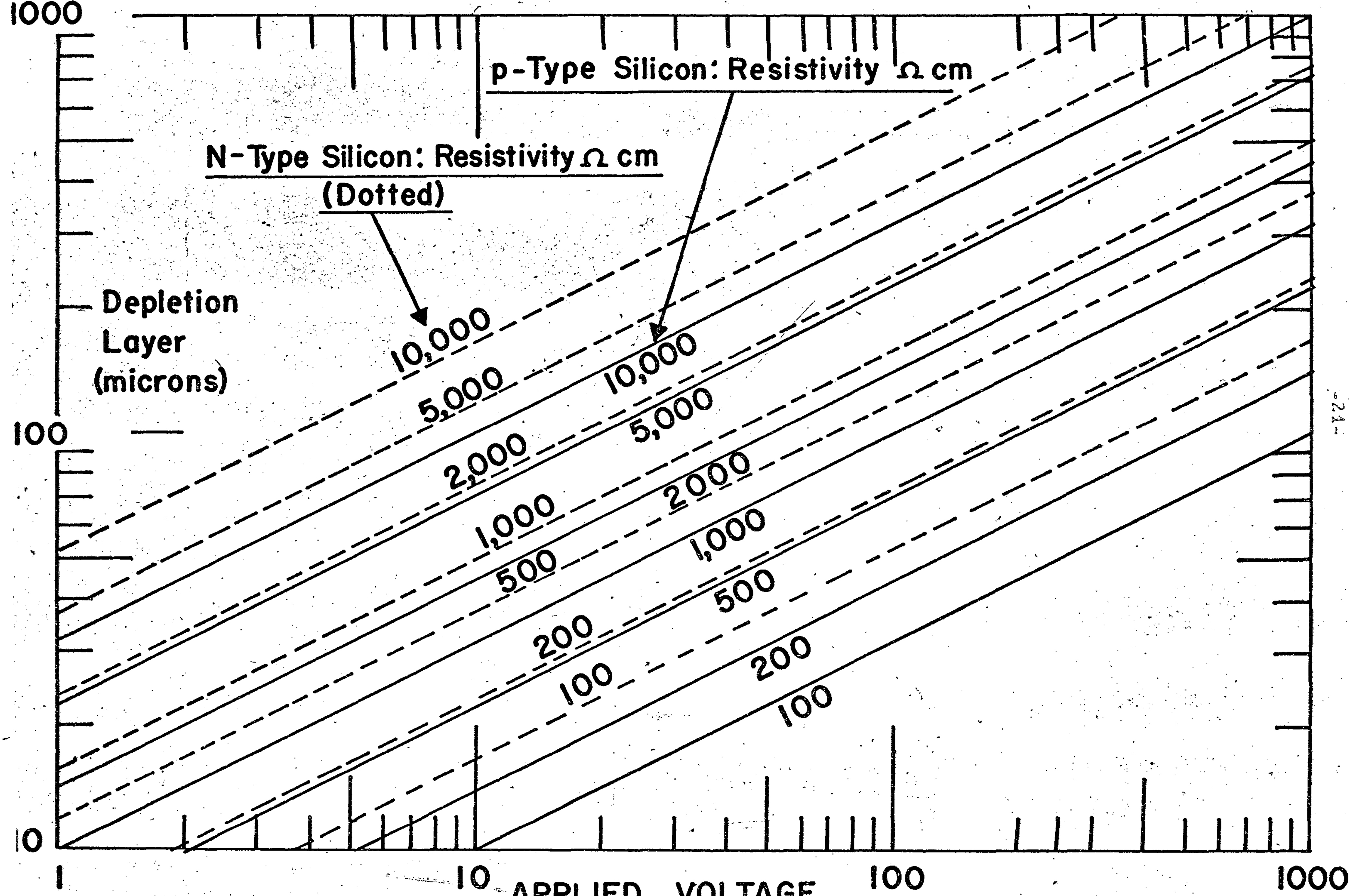
1000
100
10
Depletion
Layer
(microns)
p-Type Silicon: Resistivity Ω cm
N-Type Silicon: Resistivity Ω cm
(Dotted)
10,000
5,000
2,000
1,000
500
200
100
10,000
5,000
2000
1,000
500
200
100
1
10
100
1000
APPLIED VOLTAGE

Fig. 12

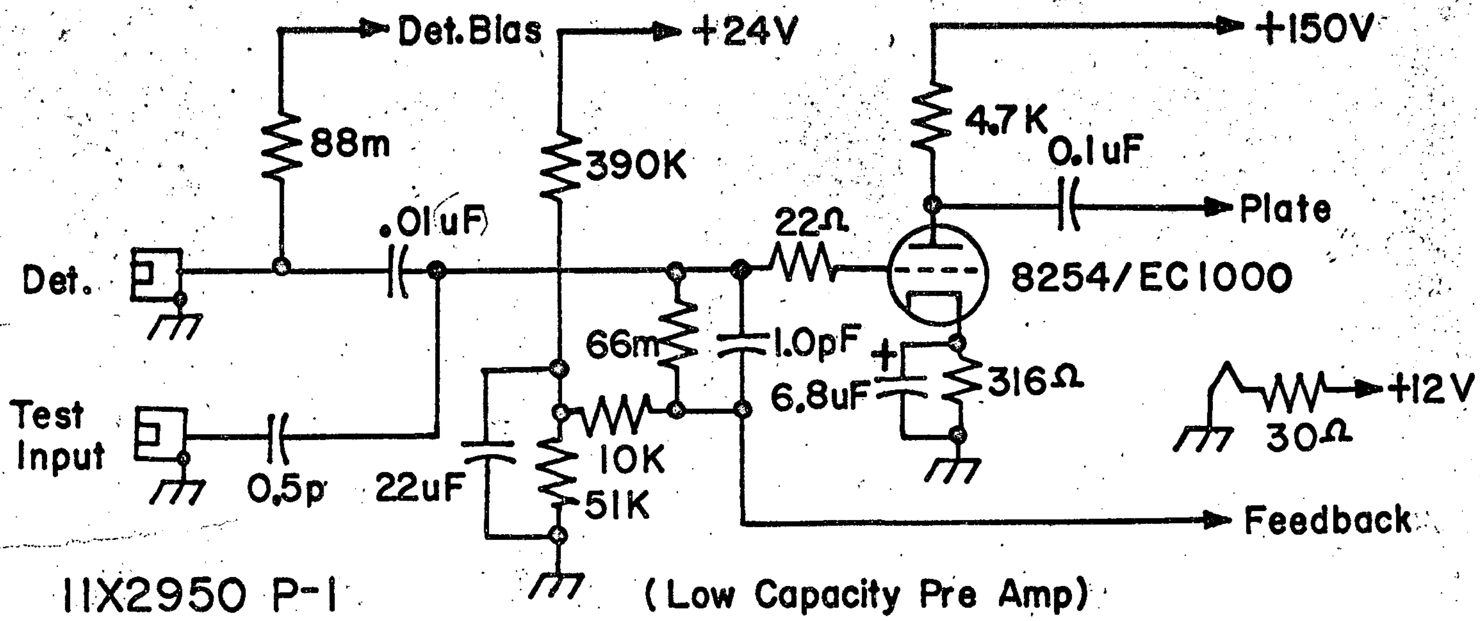

11X2950 P-1 (Low Capacity Pre Amp)

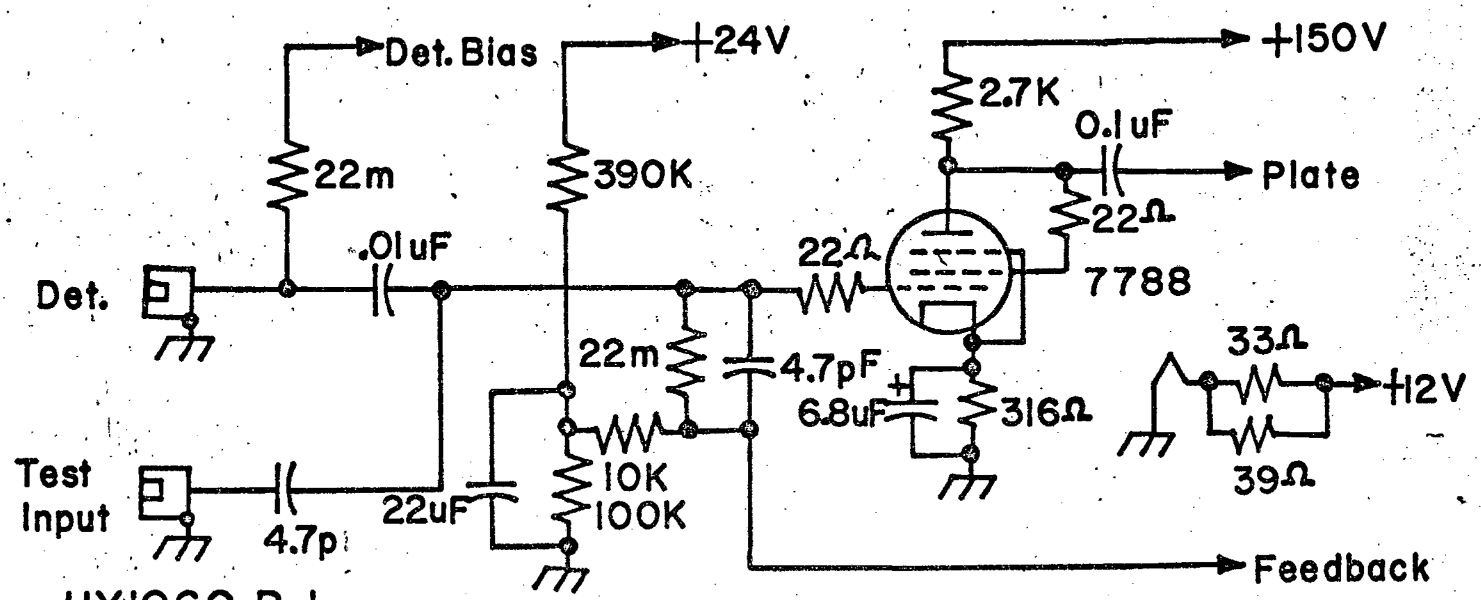

11X1060 P-1 (High Capacity Pre Amp)

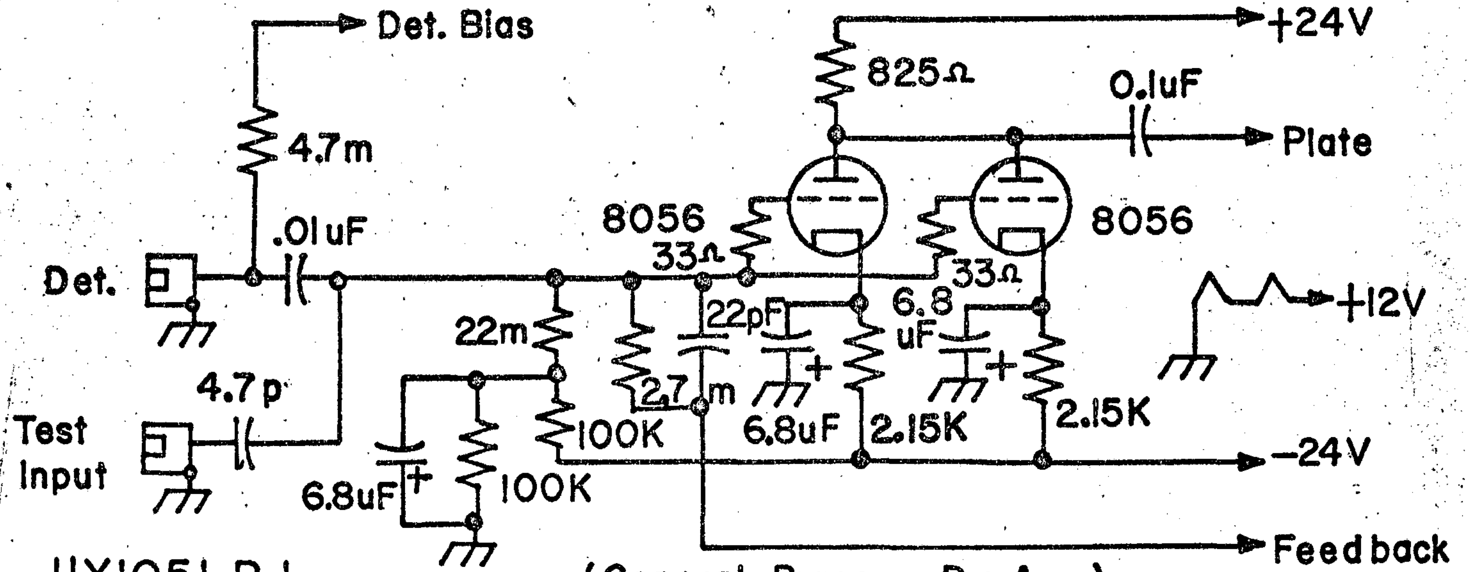

11X1051 P-1 (General Purpose Pre Amp)

Fig. 13

Pre Amp Output Circuit 11X1421 P-1

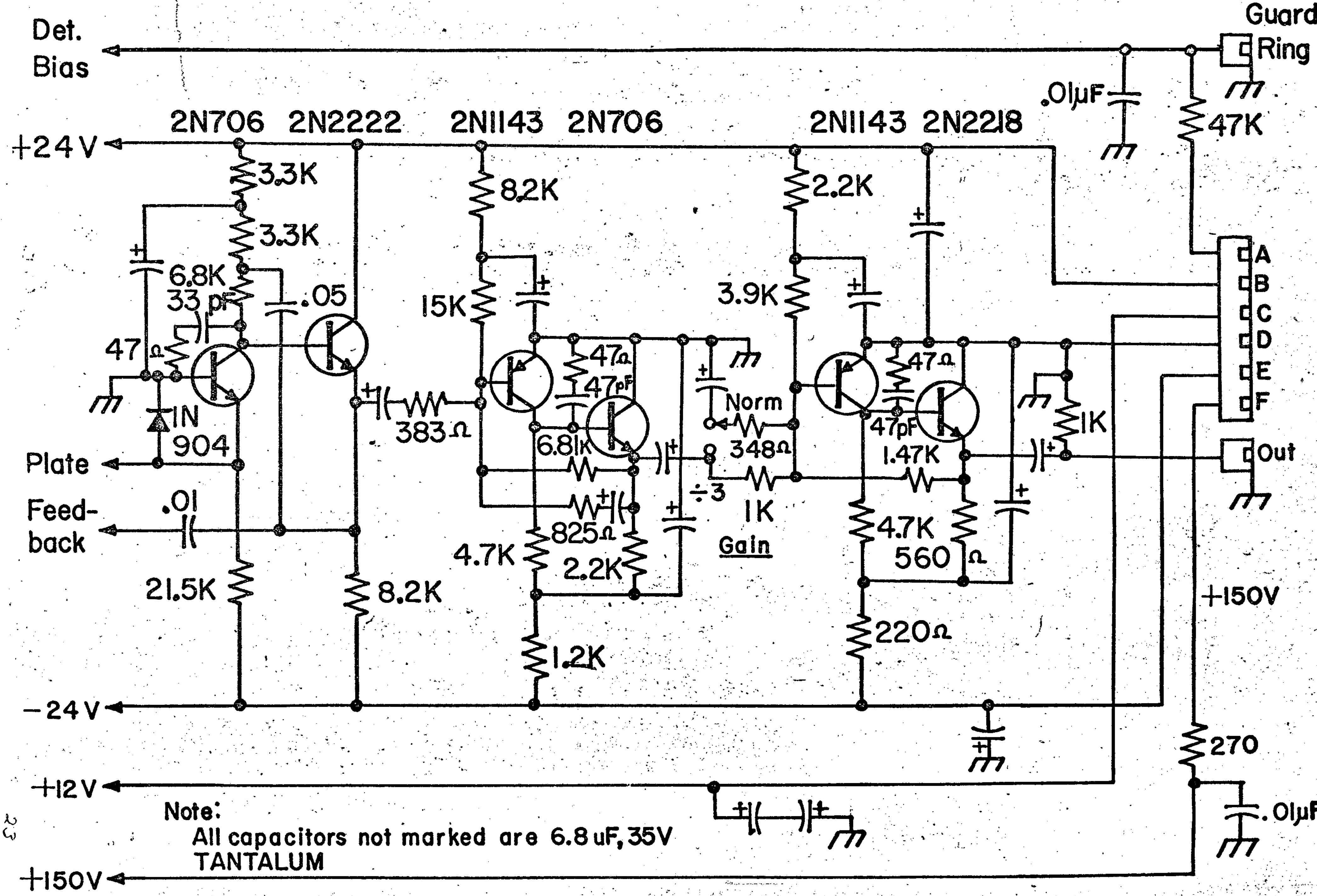

Note:
All capacitors not marked are 6.8 uF, 35V TANTALUM

Fig. 14

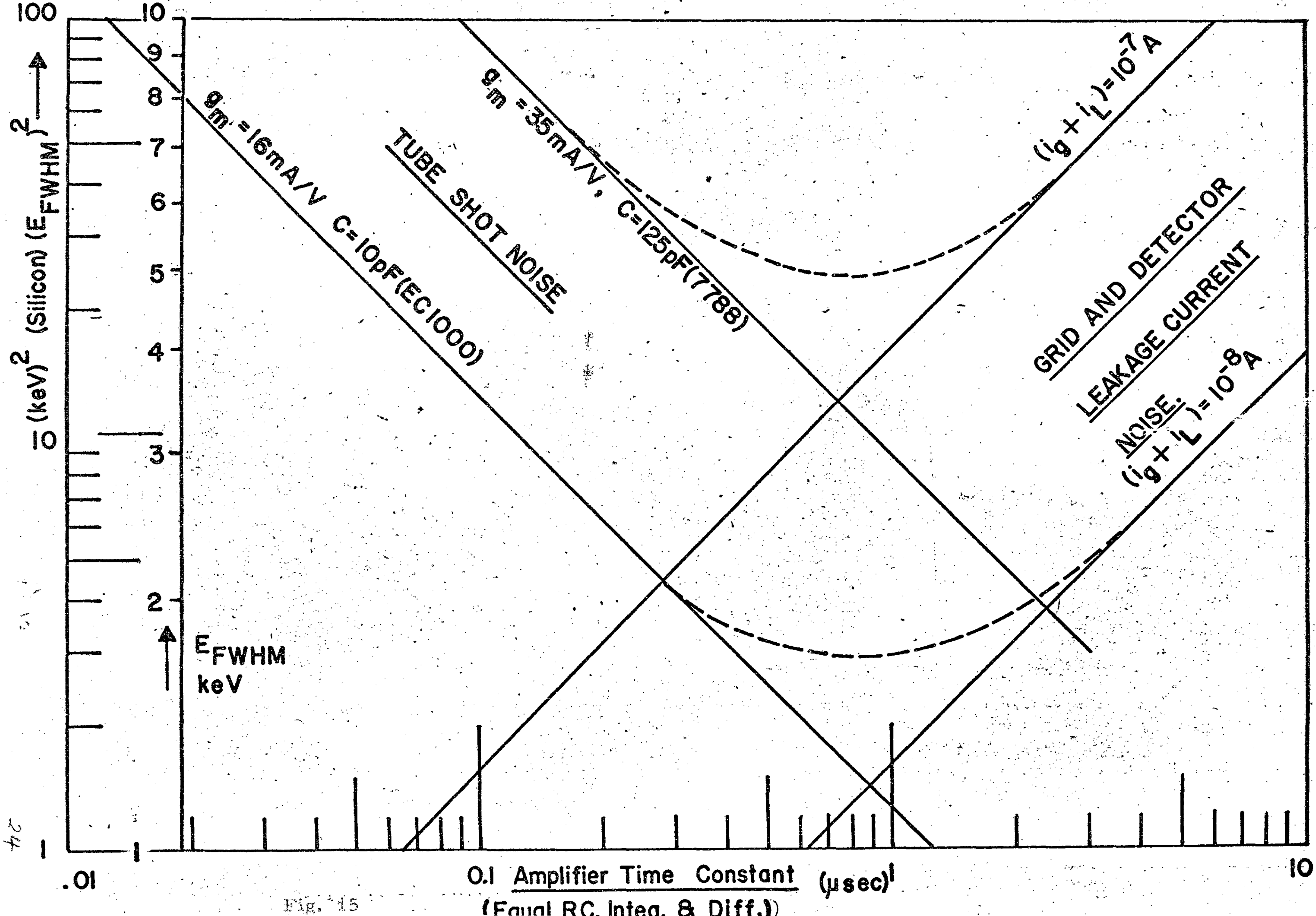
100
10
1
$(\text{keV})^2$ (Silicon) $(E_{FWHM})^2$
10
9
8
7
6
5
4
3
2
1
E_{FWHM} keV
.01
0.1
1
10
Amplifier Time Constant (μsec)
(Equal RC Integ. & Diff.)
g_m = 16mA/V C=10pF(EC1000)
g_m = 35mA/V, C=125pF(7788)
TUBE SHOT NOISE
$(i_g + i_L) = 10^{-7}$A
GRID AND DETECTOR
LEAKAGE CURRENT
NOISE:
$(i_g + i_L) = 10^{-8}$A

Fig. 15

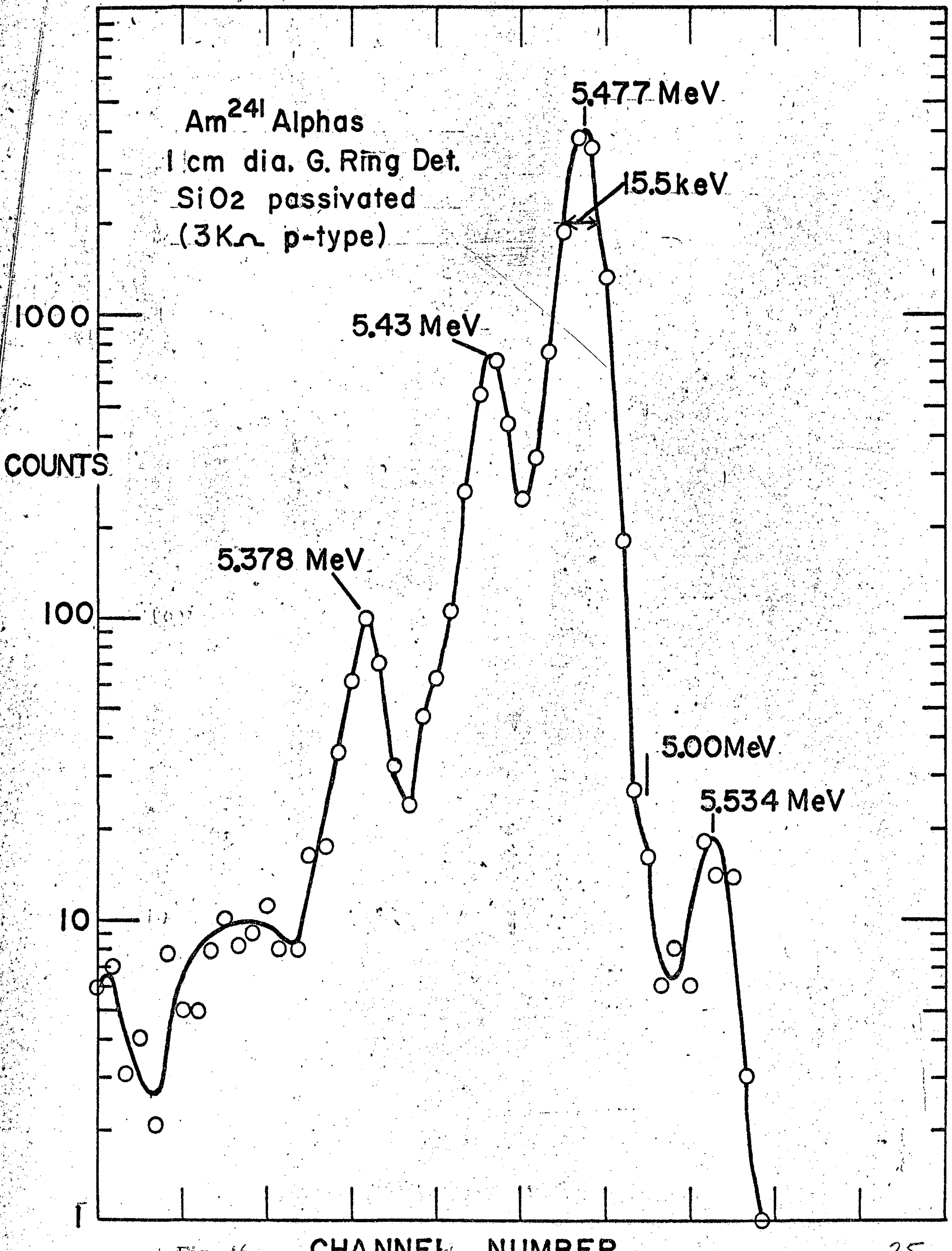
Am^{241} Alphas
1 cm dia. G. Ring Det.
SiO2 passivated
(3KΩ p-type)
5.477 MeV
15.5 keV
5.43 MeV
5.378 MeV
5.00MeV
5.534 MeV
1000
COUNTS
100
10
1
CHANNEL NUMBER

Fig. 16

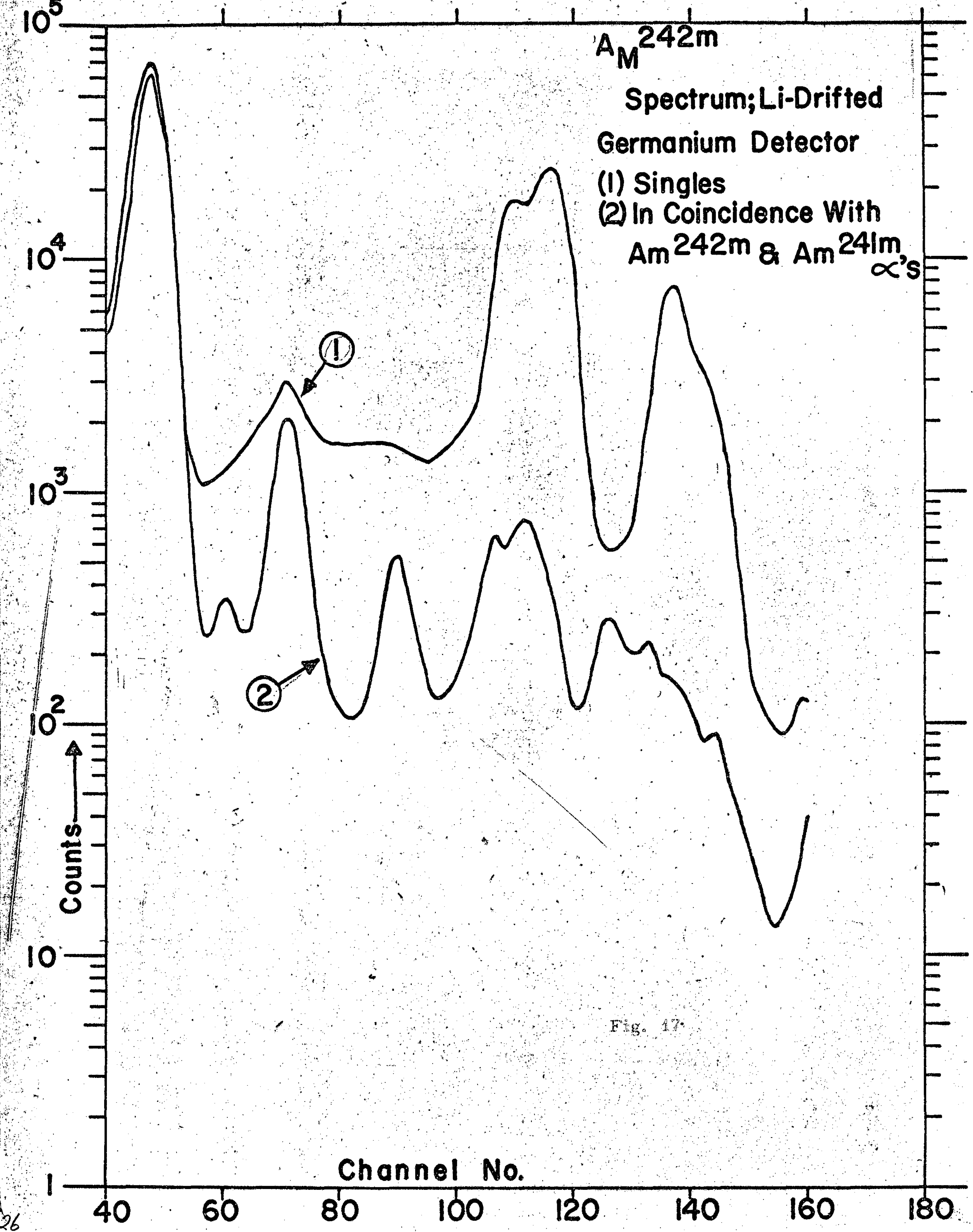

AM242m
Spectrum; Li-Drifted
Germanium Detector
(1) Singles
(2) In Coincidence With
Am242m & Am241m
α's
①
②
Counts
Channel No.
10⁵
10⁴
10³
10²
10
1
40
60
80
100
120
140
160
180

Fig. 17

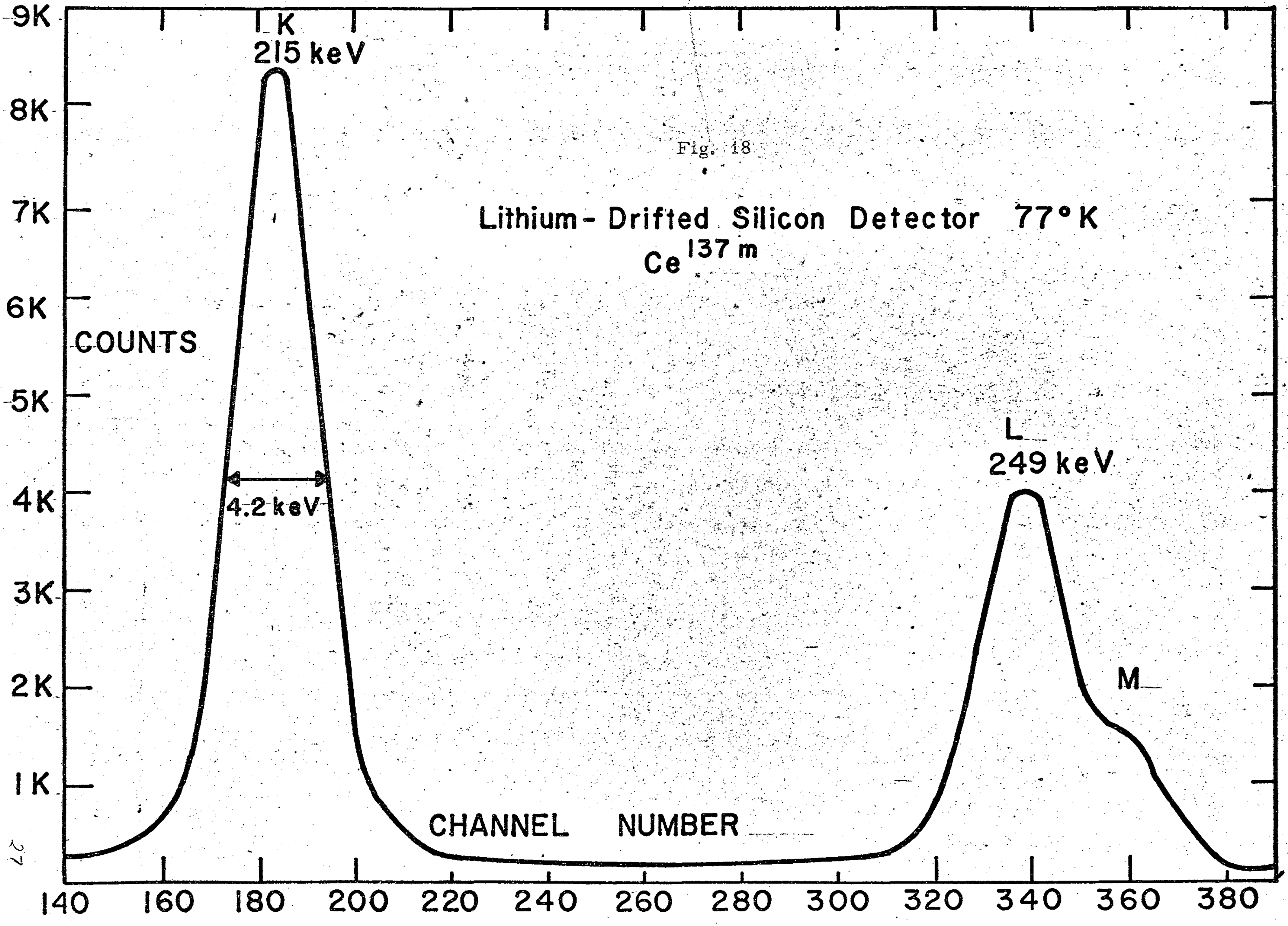
Lithium-Drifted Silicon Detector 77° K
Ce^{137m}
COUNTS
CHANNEL NUMBER
K
215 keV
4.2 keV
L
249 keV
M
9K
8K
7K
6K
5K
4K
3K
2K
1K
140
160
180
200
220
240
260
280
300
320
340
360
380

Fig. 18

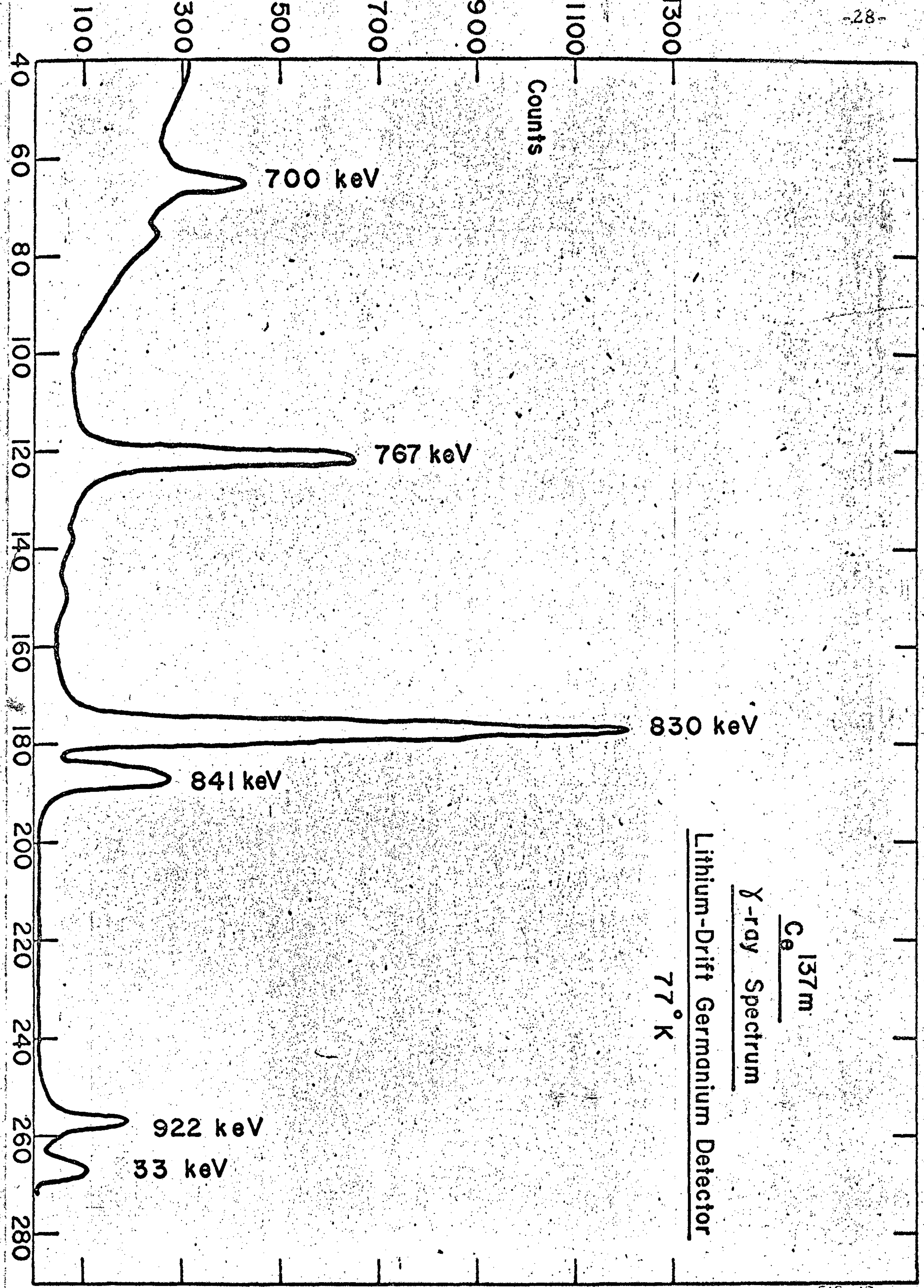
Ce137m
γ-ray Spectrum
Lithium-Drift Germanium Detector
77°K
Counts
100
300
500
700
900
1100
1300
40
60
80
100
120
140
160
180
200
220
240
260
280
700 keV
767 keV
830 keV
841 keV
922 keV
33 keV

FIG. 19

Fig. 19

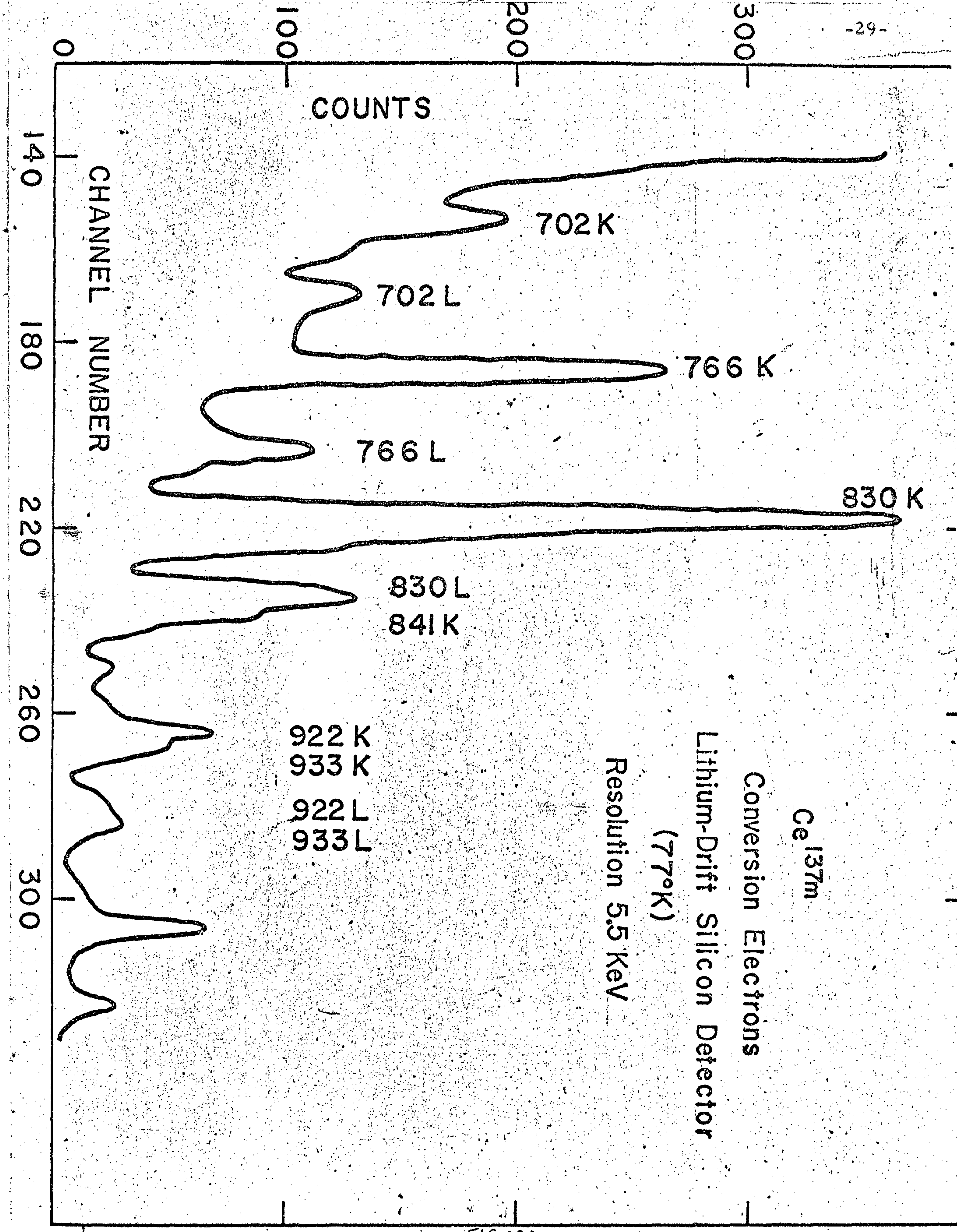
Ce^{137m}
Conversion Electrons
Lithium-Drift Silicon Detector
(77°K)
Resolution 5.5 KeV
COUNTS
0
100
200
300
CHANNEL NUMBER
140
180
220
260
300
702 K
702 L
766 K
766 L
830 K
830 L
841 K
922 K
933 K
922 L
933 L

FIG. 20

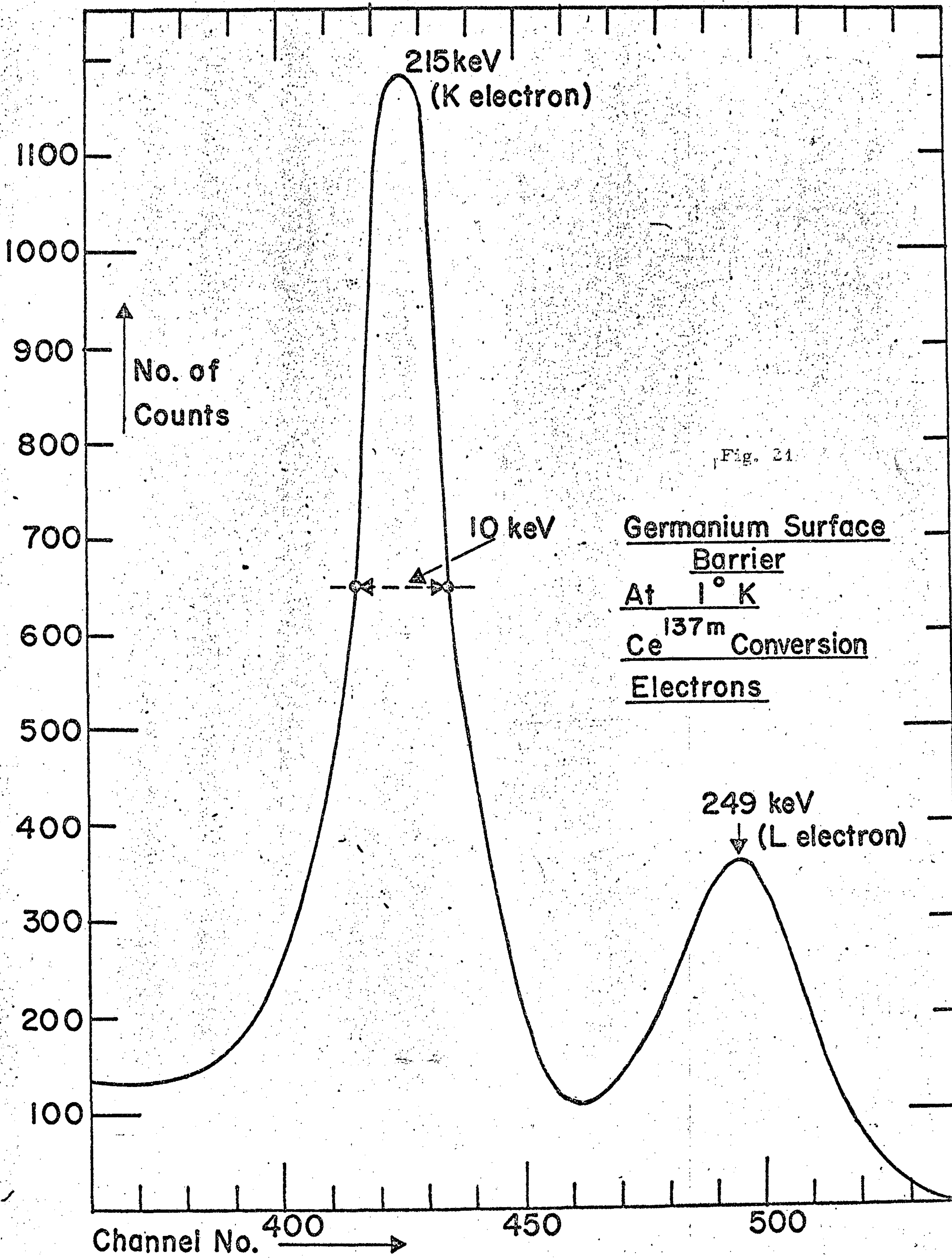
215keV
(K electron)
10 keV
249 keV
(L electron)
Germanium Surface Barrier
At 1° K
Ce^{137m} Conversion Electrons
No. of Counts
1100
1000
900
800
700
600
500
400
300
200
100
Channel No.
400
450
500

Fig. 21